School of Electrical Engineering, Computing and Mathematical Sciences (EECMS)

Adaptive Modulation Schemes for Underwater Acoustic OFDM Communication

Suchi Barua

This thesis is presented for the Degree of
Doctor of Philosophy
of
Curtin University

March 2023

Declaration

To the best of my knowledge and belief this thesis contains no material previously published by any other person except where due acknowledgement has been made.

This thesis contains no material which has been accepted for the award of any other degree or diploma in any university.

Suchi Barua

Date: 06/03/2023

Acknowledgement

First and foremost I thank to Almighty for giving me the grace and privilege to pursue my PhD, which turned out to be quite remarkable journey in spite of many challenges. Undertaking PhD has been a truly life-changing experience for me and it would not have been possible to do without the support and guidance that I received from many people.

I would like to express my heartfelt gratitude to my supervisor Professor Sven Nordholm and co-supervisor Professor Yue Rong who have been tremendous mentors for me to complete this task. A very big thank to you for your every bit of guidance, assistance, involvement and encouragement throughout the years to produce this thesis. I could not have asked for better role models, each inspirational, supportive, and patient. I could not be prouder of my academic roots and hope that I can in turn pass on the research values and the dreams that they have given to me.

I would also like to thank Dr. Narottam Das, who first recognized my research interests and helped me find numerous opportunities to accomplish my ambitions. I would like to express my gratitude towards Dr. Peng Chen who contributed to numerous discussions, experimental deployments and data collection in support of this project. I am also grateful to all my teachers

and mentors I met throughout my life who sow the seed in me for pursuing PhD and helped me to weave the dream of pursuing PhD.

During this PhD period, definitely everyday wasn't the best day. I met many nice people who were always willing to help me, cheer me up, encouraged me on those days saying that, tomorrow must be the better day. I want to thank Lara and Yuthika to make me feel the group as a family. Every moment I spent with you will be cherished forever. I really do not know how to express my gratitude to you two but best wishes to you will be always given from me.

My deep gratitude also goes to Curtin University and Curtin University Postgraduate Student Association (CUPSA) for providing the research support and student travel grant.

A special thanks to my family. Words cannot express how grateful I am to my mother, father and my sisters for supporting and encouraging me and most importantly believing in me. Your prayer for me was what sustained me thus far. I would like to express appreciation to my husband for his support during the course of this study and to darling Aarish and Aayush for being such good kids that past years and making it possible for me to complete what I started.

Suchi Barua

March 2023

List of Publications

Much of the work in this thesis has been published. These papers are:

1. S. Barua, Y. Rong, S. Nordholm, and P. Chen, "Real-time Adaptive Modulation Schemes for Underwater Acoustic OFDM Communication", *MDPI Sensors*, vol. 22, no. 3436, Apr. 2022.

2. S. Barua, Y. Rong, S. Nordholm, and P. Chen, "Real-time Subcarrier Cluster-based Adaptive Modulation for Underwater Acoustic OFDM Communications", *Proc. MTS/IEEE OCEANS*, Biloxi, Mississippi, USA, Oct. 19-22, 2020.

3. S. Barua, Y. Rong, S. Nordholm, and P. Chen, "A LabVIEW-Based Implementation of Real-Time Adaptive Modulation for Underwater Acoustic OFDM Communication", *Proc. MTS/IEEE OCEANS*, Singapore, Apr. 6-9, 2020.

4. S. Barua, Y. Rong, S. Nordholm, and P. Chen, "Adaptive Modulation for Underwater Acoustic OFDM Communication", *Proc. MTS/IEEE OCEANS*, Marseille, France, June 17-20, 2019.

To Whom It May Concern,
I, Suchi Barua, contributed to the above listed publications as indicated therein.

Suchi Barua

March 2023

Abstract

High-speed underwater communication is vitally important in many underwater applications such as off shore oil and gas industry, monitoring environmental pollution, collection of scientific data that are recorded at submersed stations, communication between submarines, divers and autonomous underwater vehicles (AUVs) and defence application. However, high data rate communication is challenging in underwater acoustic (UA) communication as UA channels vary fast according to environmental factors such as waves, currents and tides. The UA channel is known as one of the most demanding channels for reliable communication because of rapid time-variation of the channel, refractive properties of the medium, randomly varying multi-path propagation, severe fading due to limited bandwidth, and large Doppler shift due to motion.

Orthogonal frequency-division multiplexing (OFDM) has become an efficient technique for UA communication as it remarkably mitigates the multipath interference with a low computational complexity. Adaptive modulation has particularly received significant attention for UA communication systems where attained spectral efficiencies are critical since usable bandwidth is severely limited. For time-varying UA channel, self-adaptive system is an effective means of obtaining higher data rate by exploiting the knowledge of the channel state information (CSI). A real-time

OFDM based adaptive UA communication system is studied in this research employing the National Instruments (NI) LabVIEW software and NI CompactDAQ device. The objective of the proposed adaptive modulation schemes is to develop a reliable UA OFDM communication system with simple and flexible prototype design which is capable of adapting the transmission parameters in real-time based on environmental conditions to guarantee continuous connectivity and maximum performance under a fixed BER at all times.

In adaptive OFDM modulation, each subcarrier can be independently modulated or all subcarriers can be modulated in the same manner. Taking this feature of adaptive OFDM modulation into account, the frame-based and the cluster-based adaptive modulation schemes are proposed for UA OFDM communication systems in this research. The estimated received signal to noise ratio (SNR) and received cluster SNR is used as CSI for the frame-based and the cluster-based adaptive modulation system respectively and used as performance metric to choose the transmission parameters of the next transmission which are sent back to the transmitter for performing the adaptive modulation. The systems allow the adaptive allocation of subcarriers, modulation size and distribution of power for transmission to enhance the reliability of communication, guarantee continuous connectivity, improve energy efficiency and boost the data rate.

In this research, a combination of the NI CompactDAQ device and NI LabVIEW software are adopted for designing and developing real-time adaptive modulation for UA OFDM communication. The NI-based implementation offers a flexible, simplified prototype design for the system and keep the software development time short compared to digital signal processor (DSP)-based design. The performance results of the proposed real-

time adaptive modulation schemes in the tank and the river experiments are also presented and the experimental results confirm the superiority of the proposed adaptive schemes.

Contents

List of Figures

List of Tables

List of Acronym

ADSL	Asymmetric Digital Subscriber Lines
AUV	Autonomous Underwater Vehicle
BER	Bit-Error-Rate
CFO	Carrier Frequency Offset
CFR	Channel Frequency Response
CFR	Channel Frequency Response
CIR	Channel Impulse Response
CP	Cyclic Prefix
CSI	Channel State Information
DFT	Discrete Fourier Transform
DSP	Digital Signal Processor
DSSS	Direct-Sequence Spread Spectrum
FHSS	Frequency-Hopping Spread-Spectrum
FSK	Frequency-Shift Keying
GPP	General-Purpose Processor
HFM	Hyperbolic-Frequency Modulated
I/O	Input/ Output

ICI	Inter-Carrier Interference
IDFT	Inverse Discrete Fourier Transform
ISI	Inter-Symbol Interference
ISR	Intelligent Successive Refinement
LFM	Linear-Frequency-Modulated
LS	Least-Squares
MMSE	Minimum Mean-Squared Error
NI	National Instruments
OFDM	Orthogonal Frequency-Division Multiplexing
PSK	Phase-Shift Keying
RF	Radio Frequency
SNR	Signal-to-Noise Ratio
TDD	Time-Division Duplexing
UA	Underwater Acoustic
UUV	Unmanned Underwater Vehicle
ZP	Zero-Padding

Chapter 1

Introduction

High data rate communication is challenging in underwater acoustic (UA) communication as underwater channels are fast varying according to environmental conditions. In order to improve the system efficiency, adaptive modulation is considered as an attractive choice for UA communication systems. A communication system implementing adaptive modulation schemes has been developed in this research for nonstationary environments such as UA channels to improve the reliability of communication, guarantee continuous connectivity and boost the data rate. In this chapter, the background of the research is concisely discussed. The main objectives and contributions of this thesis are stated and the outline of the thesis is also given. It also covers the organization of the thesis. An overview of the current state of this research is also included in the literature review section.

1.1 Background

Two thirds of the Earth's surface are covered by water and oceans hold about 96.5 percent of all Earth's water. In recent decades, significant studies

have been conducted to explore and investigate the oceanic environment which include:

- Marine life observation,
- Water quality/pollution observation,
- Inspection of natural disasters,
- Monitoring of subsea machinery such as oil-rigs and pipelines,
- Climate change prediction and
- Naval tactical operations for coastal securities.

High-speed communication in the UA channel is vitally important for marine commercial operations, offshore oil and gas industries and defence applications [1]. Oil and gas industries carry out surveys of the seafloor before they start building subsea infrastructure. Surveys are done based on the images which are gathered by the wireless underwater nodes such as unmanned underwater vehicles (UUV), divers, autonomous underwater vehicles (AUVs). Hence, the real-time streaming capability of these non-static images between the wireless underwater nodes is required as the AUV generally sends high-rate real-time data such as sonar images to the host vessel through the UA channel. Reliable and robust underwater communication system is needed to be employed to establish a sophisticated underwater networks which is required for these applications.

Electromagnetic waves propagate only over a short distance in underwater channel and face higher attenuation compared to terrestrial communication. Hence, acoustic wave is used as the most apparent medium to empower underwater communications and UA channels are widely accepted to be "quite possibly nature's most unforgiving wireless medium".

Previously, single carrier transmission with adaptive decision feedback equalization method was employed in UA communication system which causes challenges for the channel equalizer. Multicarrier modulation i.e. orthogonal frequency-division multiplexing (OFDM) has recently become an

optimistic substitute to single-carrier systems for UA communications due to its robustness to channels that exhibit both the time dispersion and the frequency dispersion. OFDM converts a frequency selective channel into parallel frequency flat sub-channels, which significantly simplifies the receiver equalization.

Limited bandwidth and time-varying multipath propagation place significant constraints on the achievable throughput of UA communication systems. So, OFDM adaptive modulation schemes have been introduced later which help to increase the bandwidth efficiency and data rate of the UA system. In order to achieve high spectral efficiency in such non stationary environment, the adaptive modulation and coding technique is considered in this research for UA communication.

1.2 Objectives

High speed communication remains very difficult in the UA communication channel due to limited bandwidth, extended multi-path, fast time variations of the channel, refractive properties of medium, severe fading and large Doppler shifts. The extremely diverse environment makes the channel estimation and tracking very difficult. Remarkable development have been attained on UA communication in recent years in single carrier and multicarrier transmission. Nevertheless, fast varying multipath propagation and bandwidth limitation still put restriction on the achievable data rate of UA communication system. Therefore, having a good knowledge and understanding of the UA channel is very important to develop a UA communication system.

In this research, multicarrier modulation is used in the form of OFDM and adaptive modulation and coding technique is considered in order to achieve high spectral efficiency in nonstationary UA environments. The transmitter does not exploit any knowledge regarding available channel parameters in non-adaptive (fixed) modulation. On the other hand, in adaptive modulation, channel knowledge is made available to the transmitter. As a consequence, the performance of an adaptive modulation scheme relies on the transmitter's knowledge of the channel which is sent back from the receiver to the transmitter. The objective of this research is developing self-adapting algorithms for the UA communication system by analyzing the characteristics of the channel and varying transmission parameters according to the channel condition.

1.3 Contributions of the Thesis

In this research, to improve the reliability of communication and boost data rate, adaptive modulation is used that involves the selection of transmission parameters according to the channel condition. Signal-to-noise ratio (SNR) is used as the channel state information (CSI) to choose the adaptive allocation of the transmission parameters which are sent back to the transmitter for the next transmission.

The proposed adaptive scheme enables the system to perform the following:

- Adaptive allocation of the modulation order.
- Adaptive allocation of the data subcarriers.
- Adaptive allocation of the power on the data subcarriers.

The proposed adaptive modulation scheme allows the system

i. to choose a proper modulation depending on the channel conditions to improve the system throughput under a fixed bit-error-rate (BER).
ii. to discard subcarriers that experience deep fade to improve the energy efficiency of the system.
iii. to distribute the residual power among the remaining subcarriers which ensures constant transmitted symbol energy in spite of the channel variation to achieve overall better throughput of the system.

In this research, a combination of National Instruments (NI) LabVIEW software and CompactDAQ device are adopted for real-time adaptive modulation for UA OFDM communication. Compared to the digital signal processor (DSP)-based design, the proposed implementation provides simplified integration with the hardware which helps rapid acquisition and visualization of data from NI input/output (I/O) or third-party I/O devices, thus requiring less software development time. The proposed software defined implementation is flexible and simplifies the prototype design compared to conventional DSP-based design.

1.4 Thesis Outline

This thesis contains five chapters and the organization is shown in Figure 1. The thesis is organized as follows.

Chapter 1 covers the background, objectives and contribution of the research. Chapter 2 describes the theoretical model which includes the system model, UA channel model, carrier frequency offset (CFO) estimation and SNR estimation used in this research. Chapter 3 describes frame-based adaptive modulation with experimental results. Chapter 4 contains cluster-

based adaptive modulation with experimental results. Chapter 5 concludes this thesis and some suggestions are given for future work.

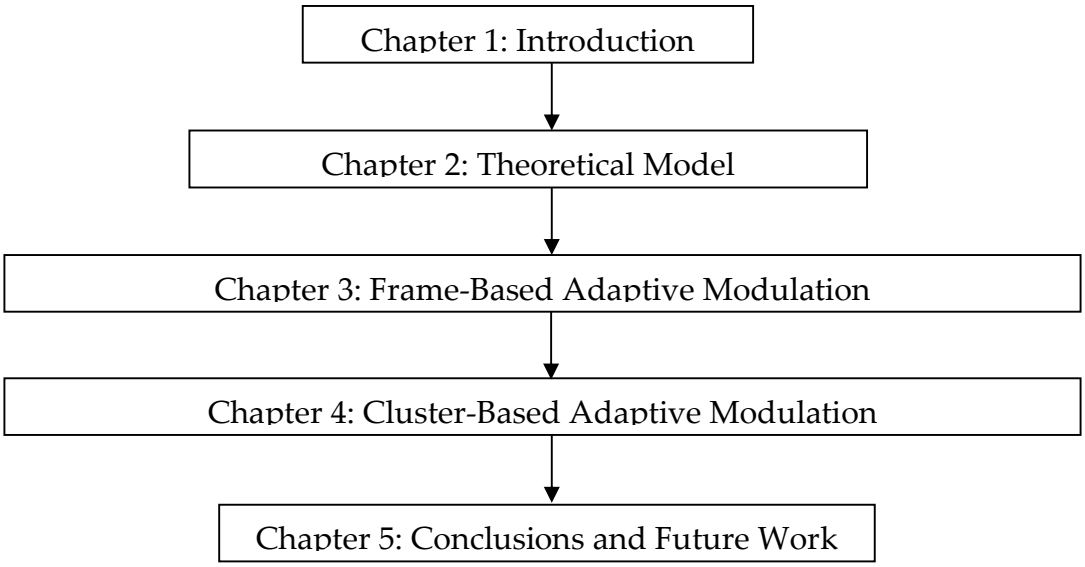

Figure 1: Organization of the chapters.

1.5 Literature Review

A growing interest has been seen for past four decades in UA communications because of its applications in marine research, oceanography, marine commercial operations, the offshore oil industry and defence. Continued research that performed over the years in UA communication system contributed in improved and robust performance of the system [1].

In underwater communications, acoustic waves are preferred over electromagnetic waves as the latter suffer from high attenuation and severe scattering in the medium of water. Due to the narrow bandwidth of the UA channel, underwater communication has low data rates compared to terrestrial communication. Sound reflection at the surface in the shallow water environment and sound refraction in the deep water environment lead

to multipath effect. In addition, relatively large delay spread is often induced by the multipath effect and the low propagation speed of acoustic wave in water. On the other hand, the movement of the instrument due to waves, currents and tides results in fast varying channel. So, underwater communication is difficult due to factors such as multipath propagation, time variations of the channel, small available bandwidth and Doppler effect due to motion.

Since late 1980s, significant amount of research has been done in UA communication with the aim of overcoming the challenges of the UA channel. Before OFDM prevails in recent years, remarkable progresses have been made in single carrier UA communication systems [2-6]. In previous works, various modulation schemes like noncoherent frequency-shift keying (FSK), coherent phase-shift keying (PSK), direct-sequence spread spectrum (DSSS) etc. have been adopted. FSK is one of the earliest forms of modulation used for acoustic modems. This is a relatively easy form of modulation and therefore used in the earliest 1980's acoustic modems. However, most incoherent communication systems yield relatively low data rates. Interest in phase coherent systems due to their higher bandwidth efficiency led to a large number of publications in the 1990's. The experimental results in [7] showed that both frequency-hopping spread-spectrum (FHSS) and DSSS performed well in two experimental scenarios.

Long range and high data rate communication in the UA channel is vitally important for marine commercial operations, offshore oil and gas industries, and defence applications. However, the UA channel is extremely bandlimited and are fast varying spatially and temporally [8-10] which poses many obstacles to enhance the data rate of UA communication system over a long distance [1, 11, 12]. For instance, in long range systems operating over

several tens of kilometres, the available bandwidth is only on the order of several kilohertz. At medium ranges (several kilometres), the available channel bandwidth is on the order of several tens of kilohertz. Only at short ranges (a few tens of metres), is the available bandwidth in excess of 100 kHz [12]. Therefore, most existing underwater acoustic communication systems are bounded by a maximum range-rate product of 40 km.kbps [11]. Such limited range-rate product is insufficient for many recent underwater applications such as AUV based seafloor survey in oil and gas industries [13]. For these applications, a larger range-rate product is required in order to transmit high-rate real-time data over a long distance. Bandwidth efficient phase coherent communications were developed three decades ago, which significantly improved the data rate compared with FSK modulation (less than 1 kbps) and achieved a data rate of 10 kbps over short ranges [11] but still often remain not as reliable and robust as desired [14].

In recent years, OFDM has been very actively pursued for UA communications [15-24] due to its resilience against frequency selective channels with long delay spreads [25]. Compared to single carrier systems, an OFDM system has advantages of low receiver complexity. By dividing the available bandwidth into a number of narrower bands, OFDM system can perform equalization in the frequency domain, thus eliminating the need for complex time-domain equalizers. A real-time implementation of OFDM in UA communication is discussed and the experimental results obtained in the shallow water at the Mediterranean Sea during trials carried out in October 2004 off La Ciotat (FR) are presented in [26]. The experiment was conducted to compare the performance of OFDM with DSSS, both using differential PSK modulation. Nevertheless the results obtained with the OFDM modulations were found well, where almost error free transmission with bit

rate equal to 800 bps was possible up to 12 km using a single transducer at the transmitter and a single hydrophone at the receiver. The authors reported the results obtained with DSSS being slightly poorer in these experimental conditions.

It can be noted that despite recent advances in UA communications, most of the published research outcomes are based on either numerical simulations or off-line signal processing of recorded data. In contrast to extensive research work, fewer studies exists on the development of real-time UA modems which include commercial products (LinkQuest, DSPComm, Subnero, Benthos). The UA modems which are broadly used in the research community [27] and experimental designs [28-31] are based on single carrier systems. Regarding UA OFDM modem development, there are even fewer work which are published in [32-36]. In [34, 37], an implementation of OFDM-based modems for UA communication using the TMS320C6713 digital DSP development board has been demonstrated. However, such DSP-based implementation can be time-consuming on system design and development [38]. In [39, 40], a real-time OFDM-based UA communication system is implemented using the NI CompactDAQ device and the LabVIEW software.

UA modem based on a DSP board and an ARM-based BeagleBone board was presented in [41]. The authors of [42] developed a reconfigurable UA modem based on a Xilinx Zynq Z-7020 system-on-chip architecture incorporating a dual ARM Cortex-A9 and an Avnet PicoZed XC7Z020-1CLG400 field-programmable gate array (FPGA). A comprehensive review of existing literature on software-defined modems for UA communications is provided in a recent work [43]. We would like to note that these DSP and FPGA based implementations can be time consuming on system hardware

and software design and implementation [43]. Compared with DSP and FPGA based designs, the NI LabVIEW implementation is more flexible and has a shorter development time. The NI CompactDAQ device combined with the LabVIEW software provide an attractive solution to simplify the prototype design and reduce the software development time compared to DSP-based implementation [39, 40].

In general, a thorough knowledge of the specific hardware and/or software architecture is needed to modify the UA modem implemented on a dedicated architecture, such as DSP or FPGA. On the contrary, there is less specialized knowledge required on systems running on general-purpose processors (GPPs). Although some of the systems in [26] are GPP-based, they do not exploit the convenient graphical programming environment of LabVIEW. Using the LAbVIEW system, researchers are relieved from programming a dedicated processor, which enables them to focus their efforts in developing high-performance UA communication algorithms. Moreover, LabVIEW provides simplified integration with hardware, which enables a rapid system configuration.

Unfortunately, using simulations or off-line processing may underestimate the challenges in real-time high speed UA communication systems. In fact, the computation complexity of signal processing algorithms for UA communication increases dramatically with data rate due to the increasing inter-symbol interference (ISI) and Doppler effect, making real-time communication more challenging. Moreover, off-line simulations are limited to recorded channel and noise data in a specific environment. In contrast, a real-time platform can be applied in more scenarios that may be encountered in practice, making a significant step towards commercial deployment of high speed UA communication systems. However, compared

with general communication systems, the following challenges posed by the harsh UA channel must be addressed before the deployment of a real-time high speed communication system.

1.5.1 CP-OFDM

In UA communication, multipath arrival causes ISI in an OFDM scheme. Introducing a guard interval between adjacent OFDM symbols is one of the most widely used method to avoid ISI. If the guard interval is longer than the delay spread of the channel, ISI is completely removed and a minor equalization is required. The guard interval is usually introduced in the form of a symbol prefix. A zero-filled symbol prefix destroys the orthogonality of the sub-carriers in the OFDM symbol. However, a cyclic prefix (CP), maintains orthogonality as well as eliminate ISI [44]. Although OFDM schemes based on zero-padding (ZP) can be developed [45], we use the CP in our implementation.

1.5.2 Doppler scale estimation

UA channels are fast-varying because of the surface motions and the unstable medium which frequently causes stretch and compression in the received waveforms, contributing large Doppler shifts on OFDM subcarriers [36, 37]. An accurate estimation of the Doppler scale factor and the subsequent frequency offset compensation is important for robust performance in real-time underwater channels to re-establish the orthogonality among the subcarriers in an OFDM signal.

The orthogonality among the subcarriers of OFDM signal enables more efficient use of total available bandwidth. For this reason, OFDM has higher

bandwidth efficiency compared with single carrier UA communication but in the presence of CFO, this orthogonality gets destroyed and system performance degrades. The speed of sound in the ocean is only around 1500 m/s. Thus, even modest speeds can produce significant Doppler shifts. For instance, a speed of 15 m/s yields a 1 percent frequency shift. Additionally, to make things worse, the speed of sound varies with temperature, salinity and pressure, resulting in significant refraction effects, especially in the vertical plane. Unfortunately, a distinct CFO is present in UA communication in most of the cases because of the continuous movement of the medium and the relatively slow propagation speed of the sound wave in water. Hence, CFO estimation is one of the important tasks for UA communication systems.

In previous works like [21, 33, 46-48], particular attention has been given to Doppler scale estimation. The CP-OFDM and ZP-OFDM structures offers many options for Doppler scale estimation [37]. Usually Doppler scale is estimated successfully by inserting waveforms which is known to the receiver during the data transmission. In one approach, a pulse train is inserted which is formed by the repetition of a Doppler-insensitive waveform, such as linear-frequency-modulated (LFM) waveform and hyperbolic-frequency modulated (HFM) waveform and in another approach, Doppler-sensitive waveform with a thumb-tack ambiguity function is used. In [47], a blind estimation with a bank of self-correlators was proposed by using the cyclic repetition structure of the CP-OFDM preamble. This approach enables accurate Doppler scale estimation compared with the LFM-based alternative. The authors of [47] also analyzed the impact of Doppler scale estimation accuracy on the system performance.

In [36], different Doppler scale estimation methods for CP-OFDM and ZP-OFDM are compared in UA communication. For a CP-OFDM preamble,

both simulations and experimental results reveal that the correlation-based methods have a decent performance in the low SNR region, and the null subcarrier based blind estimation methods can draw near or even outperform the correlation methods in the high SNR region [36]. A two-step approach is applied to the received time domain signal in [21 and 33] to reduce the Doppler effect in ZP-OFDM. First, resampling operation is executed to compensate the main frequency offset, which converts a wideband problem into a narrowband problem. After that, high-resolution uniform compensation is executed to deal with the residual Doppler, which corresponds to the narrowband model for inter-carrier interference (ICI) reduction. Null subcarriers are used to facilitate the estimation of the CFO. This high-resolution algorithm corresponds to the MUSIC-like algorithm proposed in [49] for CP-OFDM. This method is adopted in [50] for CP-OFDM for the UA communication system.

In our research, we treat the channel as having a common Doppler scaling factor on all propagation paths and apply an approach which contains high resolution uniform compensation of the residual Doppler to mitigate the Doppler effect [50]. After the CFO estimation and compensation, the time domain signal is then transformed into the frequency domain through the FFT process.

1.5.3 Channel estimation

UA channel is the most challenging channel due to its time-varying and frequency selective characteristics and these characteristics make channel estimation a difficult task for coherent OFDM underwater communication. Channel frequency response (CFR) can be estimated by pilot subcarriers that are already known to the receiver. BER performance can vary a lot according

to different type of pilot pattern (such as block, comb and scatter). Each of them is proved to work well in some certain underwater environment. Comb type pilot can track channel variation but is sensitive to frequency selective fading and have a better performance in a fast time varying channel [17].

Channel estimation can be performed based on pilot signal which is the mainstream method at present. Least-squares (LS) estimation and minimum mean-squared error (MMSE) estimation [51] are two major approaches for channel estimation. After obtaining the channel state estimation at the pilot symbols, the channel responses of all subcarriers between pilot symbols can be estimated by employing various interpolation algorithms, such as linear interpolation, second-order interpolation, spline cubic interpolation, iterative algorithms and a class of algorithms based on matching pursuit, basis pursuit [18], and so on. For the pilot data processing, in the actual work (SNR in 10dB-15dB) regardless of the LS algorithm or MMSE algorithm, its performance will not be a big difference, but the performance will be a big difference when using different channel interpolation methods in different channel delay. In the case of low delay, nonlinear interpolation can lead to better performance, but when the time delay is high, the performance of time frequency conversion interpolation will be better [52]. But the iterative algorithms and matching pursuit algorithms have high computational complexity and are only applicable for certain channel conditions [23, 52].

In our research, comb type pilot pattern is used in OFDM blocks and pilot subcarriers are used to estimate the channel. First, the LS based channel estimation at pilot subcarriers is performed. Then the CFR of the whole frequency position is estimated by linear interpolation to obtain the channel

responses of the data subcarriers based on the channel responses at the pilot subcarriers.

1.5.4 Real-time adaptive modulation

Adaptive modulation is attractive for communication systems to achieve a high bandwidth efficiency by exploiting knowledge of the channel conditions. This is particularly effective in the UA scenario, where attained spectral efficiencies are critical since the available bandwidth is extremely limited due to frequency-dependent attenuation of the UA channel. In order to increase the bandwidth efficiency of UA OFDM communication systems adaptive modulation schemes can be employed [41, 42, 46, 50-53]. Each subcarrier in OFDM systems can be modulated using different modulation schemes. Different order modulations allow different number of bits to be sent per symbol according to the channel conditions. More bits per symbol can be sent applying adaptive modulation and thus higher throughputs or better spectral efficiencies can be achieved. The use of adaptive modulation allows the UA communication system to choose the highest order modulation depending on the channel conditions.

Extensive researches on receiver designs are done with fixed modulations for UA communication whereas a limited attention has been paid on the adaptive modulation in UA communications. An OFDM-based adaptive modulation system for UA communications is proposed in [46] with the objective of maximizing the data rate where the transceiver algorithms run on the TMS320C6747 DSP core during the sea experiment. An adaptive OFDM system is proposed in [53] that maximizes the throughput under the certain target BER. In this system, power levels and the modulation sizes are determined for OFDM subcarriers by using the channel

prediction information. The performance results of the sea trial are also presented with feedback implemented from a radio frequency (RF) link [53]. In [54], a single carrier PSK based adaptive modulation system is proposed, where both the modulation size and turbo code rate are adaptable. In [55], a Nakagami-m distribution has been adopted to simulate the channel behaviour of real data sets which satisfactorily captured the statistics of the channel and then used to derive the performance of the adaptive modulation scheme based on instantaneous SNR information.

In our proposed system, subcarriers, modulation size and the transmission power are adaptively allocated. Different modulation size (bit) and power allocation algorithms had been proposed for OFDM system [56, 57] and UA OFDM system [42, 53-55, 58]. The algorithm proposed in [56] adjusts the constellation size as well as the input energy which has significant implementation advantages over the well-known water pouring method in the asymmetric digital subscriber lines (ADSL) transmission environment but unfortunately it doesn't always give the optimal solution [57]. In [57], an intelligent successive refinement (ISR) algorithm is proposed for adaptively tracking the power and bit allocation for OFDM systems in a time varying channel. It also shows that, a greedy approach which successively refines the bit allocation to lower the transmit power always converges to the optimal solution. In [58], the transmitter distributes more power, when SNR of the channel is high and vice versa. The transmission power and rate are adapted by the water-filling allocation method. In [42, 53] both modulation size and power level were allocated to each subcarrier based on a greedy algorithm.

In our research, both frame-based and cluster-based adaptive modulation schemes are developed. In the frame-based scheme, all the

subcarriers are modulated and demodulated in the same manner. Hence, only modulation size is adaptively allocated in our proposed frame-based modulation scheme.

In adaptive OFDM modulation, each subcarrier can be independently modulated which leads to higher computational complexity and feedback load. This is why, the subcarriers of an OFDM frame are divided into groups of subcarriers i.e. clusters and each cluster is modulated independently rather than each subcarrier which reduces the computational complexity and feedback load of the adaptive scheme [53]. In cluster-based modulation scheme, modulation size as well as subcarriers and power are also adaptively adjusted.

In our proposed cluster-based adaptive modulation scheme, subcarriers that experience deep fade are discarded following a decision tree which is explained in Chapter four and the remaining subcarriers are allocated for transmission. In both frame-based and cluster-based adaptive modulation schemes, modulation size is adaptively allocated based on the decision tables which are included in Chapters three and four. These decision tables are determined based on the results of fixed modulation for different modulations e.g. BPSK, QPSK and 16QAM. In the cluster-based adaptive modulation scheme, power is also adaptively distributed among the clusters. As deep faded subcarriers are discarded (zero power is allocated) in this scheme, the total transmission power is reduced for the next transmission which affects the overall throughput of the system. The distribution of the residual power among the remaining data subcarriers guarantees constant transmitted symbol energy in spite of the channel variation which ensures overall better throughput of the system.

In our proposed system, real-time adaptive modulation for UA OFDM communication system has been developed and implemented using the NI CompactDAQ device and the LabVIEW software which is flexible and simplifies the prototype design compared to conventional DSP-based designs. Received SNR is chosen as the performance metric for mode switching which reflects the channel variation as well as Doppler effects. The proposed adaptive system improves energy efficiency, guarantees continuous connectivity and ensures higher data rate for a nonstationary time-varying UA channel.

Chapter 2

Theoretical Model

As electromagnetic wave propagates poorly and has very high attenuation in water, the acoustic wave is widely used for underwater wireless communications due to its low attenuation characteristic in water [12, 16]. UA communication is challenging due to unique channel characteristics such as fading, extended multipath and refractive properties of the UA channel [12, 43]. The robustness of OFDM against large multipath spread has attracted great interests from researchers in the field of UA communication [59]. The major constraint in applying OFDM to UA channels is the motion induced Doppler shift which creates non-uniform frequency offset in a wideband acoustic signal [16, 53]. A brief description of the UA channel and the OFDM technique are given in this chapter. It also contains system model, CFO estimation, channel estimation and SNR estimation which is the core of the proposed adaptive modulation schemes.

2.1 UA Channel

Underwater communications has been very challenging due to unique channel characteristics [12]. Three alternatives such as electromagnetic wave,

optical wave and acoustic wave can be considered to establish underwater wireless communication. Electromagnetic wave cannot propagate over long distances and has very high attenuation in water. Optical wave supports a high propagation speed with wide bandwidth, but the effective communication range under water does not exceed 100 m [60]. So, acoustic wave is the only feasible means of long distance underwater communication as it supports a communication range over several kilometres with low power loss [60].

The accessible bandwidth available for UA communication is limited as high frequency sounds are absorbed strongly by sea water. In a shallow water environment, where the transmission distance is larger than the water depth, wave reflections from the surface and the bottom generate multiple arrivals of the same signal. The slow propagation speed (1500 m/s) of acoustic waves and significant multipath phenomena cause very large channel delay spread. The large delay spread leads to severe ISI [25]. Time variability is one of the most challenging features of UA channel. The different time variabilities lead to different Doppler scaling effects or Doppler shifts of the transmitted signal [25]. Sound refraction in the water results frequency selective fading. Moreover, the channel impulse response (CIR) has a sparse structure which means most of the channel energy is concentrated in few paths. Figure 2 shows the multipath propagation in UA channel.

In summary, randomly varying multi-path propagation, rapid time-variation, severe fading due to limited bandwidth, refractive properties of the medium and large Doppler shifts due to motion are the main constraints for reliable communication through the UA channel [11, 12, 15, 25, 51]. Therefore, it is important to have a good understanding of channel for

designing and simulating of an underwater communication system [8, 51, 61-63].

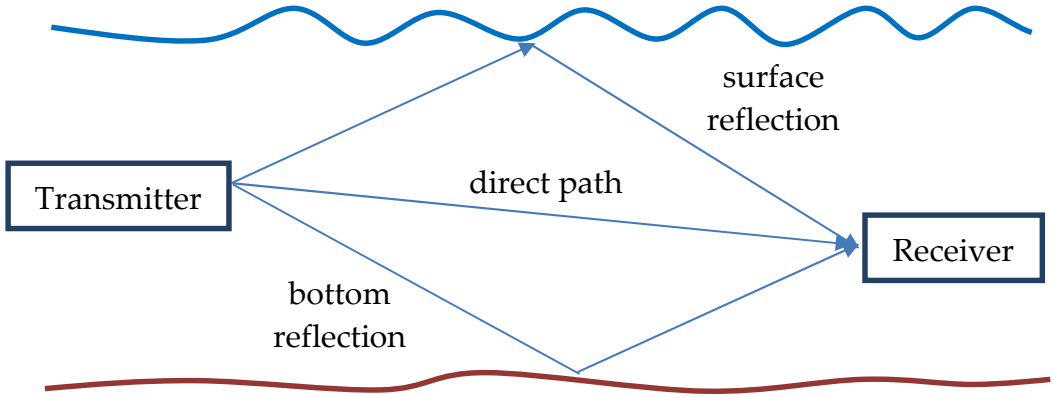

Figure 2: Multiple propagation paths in UA channel.

2.2 OFDM

The UA channel is band-limited and reverberant. The reverberant and time-varying nature of the UA channel poses many obstacles to achieve a reliable and high data-rate communications [64]. Earlier, coherent UA communication system was developed with single carrier transmission and adaptive decision feedback equalization. This approach poses great challenges for the equalizer. Multi-carrier modulation i.e. OFDM offers an alternative to a broadband single-carrier communication. The idea of multicarrier modulation is to divide the available bandwidth into a number of subbands. By dividing the available bandwidth into a number of narrower bands, OFDM systems can perform equalization in the frequency domain and eliminate the need for complex time-domain equalizers [25, 65].

OFDM has been adopted in radio communication systems as an efficient technique for high data rate transmission in frequency-selective channels [15]. OFDM has now been recognized as an appealing solution for

high data rate communications over UA channels due to their robustness against large multipath spread. The key foundation of OFDM is that the modulated symbols transmit over different subcarriers do not interfere with each other in time-invariant channels. However, in UA channels, the Doppler effect is usually very significant due to the transmitter/receiver motion and ocean waves, which results in fast time-variation. The time-variation of UA channels would then destroy the orthogonality among the subcarriers and lead to ICI.

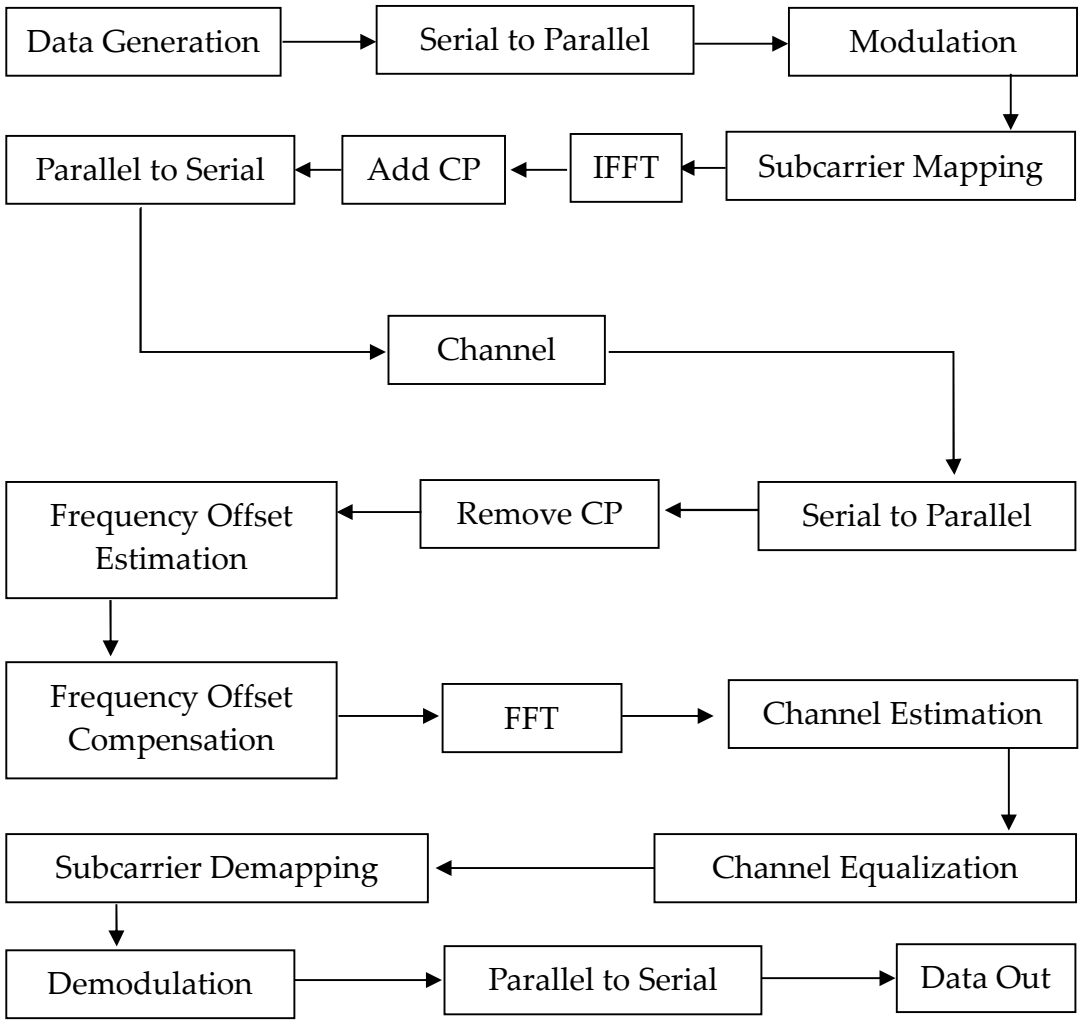

Figure 3: System block diagram of OFDM system.

An accurate estimation and compensation of CFO can reduce the ICI problem. Communications in a time-varying multipath channel suffer from the ISI which causes severe signal distortion and results in performance degradation in high data rate systems. In OFDM system, a guard interval is introduced to reduce the ISI due to multipath propagation. This is most often based on insertion of a CP [15]. Figure 3 shows the system block diagram of an OFDM system. It can be seen that, the OFDM transmitter consists of bit generation, modulation, mapping, IFFT and CP addition. The OFDM receiver is followed by reverse modules of the transmitter. In the receiver, the CP is removed. Then the CFO is estimated and frequency offset compensation is performed. After compensating the frequency offset, the receiver performs FFT, channel estimation, channel equalization, demapping and demodulation.

2.2.1 Subcarriers Assignment

In our system, three types of subcarriers are used for OFDM transmissions, which are used for different purposes.

- Pilot subcarriers are used for channel estimation.
- Data subcarriers are used to carry information symbols.
- Null subcarriers are used at the edge of the frequency band to prevent spectrum leakage. Also, null subcarriers are mixed with active subcarriers (pilot and data subcarriers) to facilitate Doppler estimation and noise variance estimation.

Figure 4 shows the subcarrier assignment of the OFDM transmission where the positions of the different subcarriers are seen in the OFDM blocks. The number of each type of subcarriers are given later in Table 2.

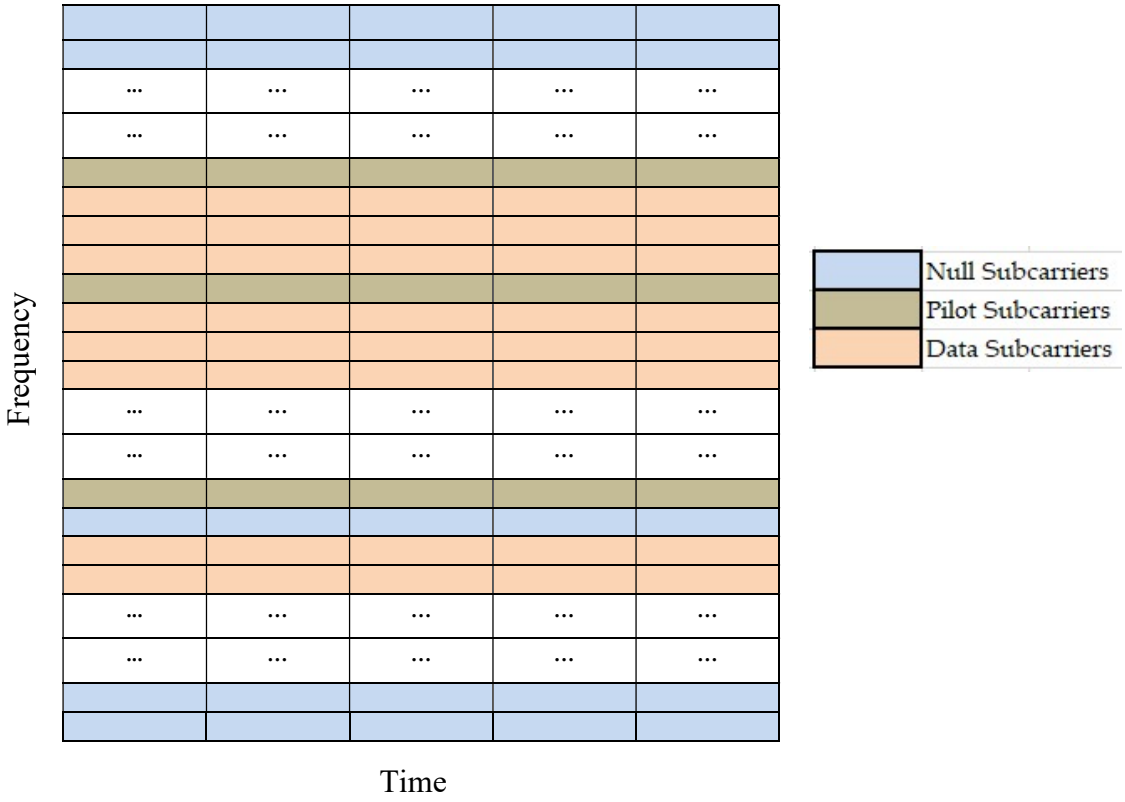

Figure 4: Subcarriers assignment for OFDM transmission.

2.3 System Model

In our research, we consider a frame-based coded UA OFDM communication system. The frame structure of the transmitted signal is shown in Figure 5. Each block contains pilot subcarriers, null subcarriers and data subcarriers. We assume that pilot subcarriers are uniformly spaced [39, 40, 66, 67]. Preamble is introduced for the purpose of synchronization.

One Frame

Preamble	Block 1	Block 2	Block 3	Block 4	Block 5	Preamble	Block 1

Figure 5: Frame structure of the UA OFDM system.

Let us introduce K_p as the number of pilot subcarriers, K_d as the number of data subcarriers, K_n as the number of null subcarriers. In each frame, a binary source data stream $\boldsymbol{b}$ is generated

$$\boldsymbol{b} = (b[1], \dots, b[K_b])^T \tag{1}$$

where $(\cdot)^T$ denotes the matrix (vector) transpose, $K_b = M\, K_d\, K_{blk}$ is the number of information-carrying bits in each frame, M denotes the modulation order (e.g. 1 for BPSK, 2 for QPSK and 4 for 16QAM) and K_{blk} denotes the number of OFDM blocks in one frame.

Then the OFDM symbol vector $\boldsymbol{s}$ is mapped from $\boldsymbol{b}$ depending on modulation constellations

$$\boldsymbol{s} = (s[1], \dots, s[K_s])^T \tag{2}$$

where $K_s = K_p + K_d + K_n$ is the number of total subcarriers. Each OFDM symbol is converted to the time domain by the inverse discrete Fourier transform (IDFT), leading to the following baseband discrete time signal

$$\boldsymbol{x} = \boldsymbol{F}^H \boldsymbol{s} \tag{3}$$

where $(\cdot)^H$ denotes the conjugate transpose and $\boldsymbol{F}$ is a $K_s \times K_s$ discrete Fourier transform (DFT) matrix with the (i,k)–th entry of $1/\sqrt{K_s} e^{-j2\pi(i-1)(k-1)/K_s}$, $i,k = 1, \dots, K_s$. Passband signals are directly generated for each OFDM block at the transmitter. The bandwidth of the transmitted signal is $B = f_{sc} K_s$, where f_{sc} is the subcarrier spacing. The duration of one OFDM symbol is $T = 1/f_{sc}$. The K_s subcarriers are located at frequencies of

$$f_k = f_c + k\, f_{sc}, \qquad k = -\frac{K_s}{2} + 1, \dots, \frac{K_s}{2}$$

where f_c is the center frequency. To avoid interference among OFDM blocks, a CP of length T_{cp} is prepended to the OFDM symbol, and the total length of

one OFDM block is $T_{total} = T + T_{cp}$. The continuous time representation of an OFDM block can be expressed as

$$\begin{aligned} \tilde{x}(t) &= 2\,\mathbb{R}\left\{\left[\frac{1}{\sqrt{K_s}}\sum_{-\frac{K_s}{2}+1}^{\frac{K_s}{2}} \check{s}[k]e^{j2\pi k f_{sc} t}\right] e^{j2\pi f_c t}\right\}, \quad 0 \le t \le T \\ \tilde{x}(t) &= \tilde{x}(t+T), \qquad\qquad -T_{cp} \le t < 0 \end{aligned} \tag{4}$$

where $\mathbb{R}\{\cdot\}$ denotes the real part of a complex number and

$$\check{s}[k] = \begin{cases} s[k], & 1 \le k \le \frac{K_s}{2} \\ s[k+K_s], & -\frac{K_s}{2}+1 \le k \le 0 \end{cases} .$$

A general UA channel with N_p paths can be represented as

$$h(t,\tau) = \sum_{p=1}^{N_p} A_p(t)\delta(t-\tau_p(t)) \tag{5}$$

where N_p is the number of propagation path, $\delta(.)$ is the Dirac delta function and t is the time at which the channel is observed. The coefficient $A_p(t)$ and $\tau_p(t)$ represent the amplitude and delay of the p th path respectively [8, 61, 66].

In general, UA communication suffers from time-varying frequency offset caused by the change of $\tau_p(t)$ within one OFDM block. In the following, we assume that $A_p(t)$ is constant and all paths have the same Doppler scaling factor ϵ during one OFDM block. Thus

$$\tau_p(t) \approx \tau_p - \epsilon t\,, \quad p = 1, \dots, N_p\,.$$

Then the received passband signal of one OFDM block is given by

$$\tilde{r}(t) = \sum_{p=1}^{N_p} A_p \, \tilde{x}\,(t - \tau_p + \epsilon t) + \tilde{w}(t) \tag{6}$$

where $\tilde{w}(t)$ is the passband additive noise. Then the Doppler scaling factor is estimated. After removing the CP, downshifting, and low-pass filtering $\tilde{r}(t)$, the baseband received signal can be obtained from (4) and (6) as

$$\begin{aligned} r(t) &\approx e^{j2\pi\,\check{\epsilon} t} \sum_{p=1}^{N_p} \frac{A_p e^{-j2\pi f_c \tau_p}}{\sqrt{K_s}} \sum_{k=-\frac{K_s}{2}+1}^{\frac{K_s}{2}} \check{s}[k]\, e^{j2\pi k f_{sc}(t-\tau_p)} + w(t) \\ &= e^{j2\pi\,\check{\epsilon} t} \frac{1}{\sqrt{K_s}} \sum_{k=-\frac{K_s}{2}+1}^{\frac{K_s}{2}} \check{s}[k]\, e^{j2\pi k f_{sc} t} \sum_{p=1}^{N_p} A_p e^{-j2\pi f_k \tau_p} \\ &\quad + w(t),\ 0 \le t \le T \end{aligned} \tag{7}$$

where $\check{\epsilon}$ represents the CFO introduced by the remaining Doppler shift, $w(t)$ is the baseband additive noise. From (7), the channel frequency response (CFR) at the k –th subcarrier is given by

$$H[k] = \sum_{p=1}^{N_p} A_p \, e^{-j2\pi f_k \tau_p}, \quad k = -\frac{K_s}{2} + 1, \ldots, \frac{K_s}{2} \quad . \tag{8}$$

By sampling $r(t)$ at the rate of $1/B$, we obtain discrete time samples of one OFDM symbol from (7) as

$$\begin{aligned} r[i] &= \frac{e^{j2\pi i\,\check{\epsilon}/B}}{\sqrt{K_s}} \sum_{k=-\frac{K_s}{2}+1}^{\frac{K_s}{2}} \check{s}[k]\, e^{j2\pi i k\ sc/B}\, H[k] + w[i] \\ &= \frac{e^{j2\pi i\,\check{\epsilon}/B}}{\sqrt{K_s}} \sum_{k=-\frac{K_s}{2}+1}^{\frac{K_s}{2}} \check{s}[k]\, e^{j2\pi i k/K_s}\, H[k] + w[i] \\ &\qquad\qquad\qquad\qquad\qquad\qquad i = 1, \ldots, K_s \end{aligned} \tag{9}$$

where $w[i]$ is the noise sample. The matrix-vector form of (9) is given by

$$\boldsymbol{r}_t = \boldsymbol{P}\boldsymbol{F}^H\boldsymbol{S}\boldsymbol{F}\boldsymbol{h}_t + \boldsymbol{w}_t \tag{10}$$

where

$$\boldsymbol{r}_t = (r[1], \dots r[K_s])^T$$

$$\boldsymbol{w}_t = (w[1], \dots w[K_s])^T$$

$$\boldsymbol{P} = diag\ (1, e^{-j2\pi\,\check{\epsilon}/B}, \dots, e^{-j2\pi(K_s-1)\,\check{\epsilon}/B})$$

$\boldsymbol{S}$ = diag ($\boldsymbol{s}$) is a diagonal matrix taking $\boldsymbol{s}$ as the main diagonal elements, $\boldsymbol{h}_t$ is the discrete time domain representation of the CIR with a maximum delay of $\boldsymbol{N}_m = \left\lfloor B\tau_{N_p} \right\rfloor$. After estimating and removing the CFO which will be discussed in the next subsection, the frequency domain representation of the received signal is

$$\boldsymbol{r}_f = \boldsymbol{S}\boldsymbol{h}_f + \boldsymbol{w}_f \tag{11}$$

where $\boldsymbol{w}_f$ is the additive noise vector in the frequency domain.

$$\boldsymbol{h}_f = (h_f[1], \dots . h_f[K_s])^T$$

is a vector containing the CFR at all K_s subcarriers with

$$h_f[k] = \begin{cases} H[k], & 1 \le k \le \dfrac{K_s}{2} \\ H[k-K_s], & \dfrac{K_s}{2} + 1 \le k \le K_s \end{cases} .$$

2.3.1 Synchronization

At the receiver side, the synchronization operation is performed first. The preamble block is used for the purpose of synchronization and frame head detection. For real-time experiment, the preamble block contains an N_{pn} = 127 long pseudo noise (PN) sequence followed by N_{pn} zeros. The received signal samples are first passed through a passband filter and converted from passband to baseband. Then the carrier frequency of the filtered signal is removed and finally the signal is passed

through a low-pass filter. Then the system calculates the DFT-based cross-correlation between the baseband signals and the local synchronization sequence to detect the frame head. Then the received signal is sampled at a rate of B. After removing the CP, the baseband discrete time samples of one OFDM symbol is given by equation (10).

2.3.2 CFO Estimation

In underwater communications, due to the effects of wind and currents, the relative motion between a drifting transmitter and receiver can reach a few meters per second even under mild weather conditions. The platform motions and the medium instability leads to a fast varying UA channel. Considering that slow velocity of sound in water, such motion generates strong Doppler effects [68]. OFDM is sensitive to the motion induced Doppler shift which creates non-uniform frequency offset in a wideband acoustic signal [16]. The CFO destroys the orthogonality among subcarriers and degrades the BER performance severely. CFO estimation and compensation have vital importance for robust system performance.

Doppler shift is a constraint in UA communication which leads to ICI because signal components from one subcarrier spill over to the immediate neighbouring subcarriers. With the increase of Doppler frequency, the ICI increases the power of the received signal on inactive subcarriers. As a result the possibility of erroneous detection of subcarriers state enhances and in turn misleads the detection of transmitted symbols on the active subcarriers.

In this research, it is assumed that the motion of the transmitter and/or the receiver causes the dominant Doppler shift and the channel has a common Doppler scaling factor on all propagation paths [69]. In general, different paths could have different Doppler scaling factors. When this is not the case, part of useful signals are treated as additive noise, which could

increase the overall noise variance considerably. However, it is found that as long as the dominant Doppler shift is caused by the direct transmitter/receiver motion, this assumption seems to be justified [21].

An approach is used for CFO, $\check{\epsilon}$ estimation which contains a high-resolution uniform residual Doppler compensation by null subcarriers [50]. After removing CP from the received signal, CFO is estimated in null subcarriers at the receiver side. The CFO is performed in each OFDM block. The energy of the null subcarriers is used as the cost function as

$$J(\epsilon) = |\mathbf{\Theta F \Gamma}^H(\check{\epsilon})\boldsymbol{r}_t|^2 \tag{12}$$

where $\mathbf{\Theta}$ is a selection matrix that picks the frequency-domain measurements on the null subcarriers out of all K_s subcarriers, $|\ |$ is the Euclidean norm of a vector.

$$\mathbf{\Gamma}(\epsilon) = diag\ (1, e^{j2\pi T_c \check{\epsilon}}, \dots, e^{j2\pi T_c (K_s-1)\check{\epsilon}})$$

is diagonal matrix where $T_c = 1/B$ is the time interval for each sample and $(.)^H$ denotes the complex conjugate transpose operation of a matrix. An estimation of ϵ is found through

$$\hat{\epsilon} = argmin\, J(\epsilon) \tag{13}$$

which is solved via 1-D search [21, 50]. Without the CFO fine tuning, the receiver performance would deteriorate considerably. After CFO compensation, the ICI induced by CFO is greatly reduced. ICI-free reception can be approximately achieved with this high-resolution algorithm which is similar to the MUSIC-like algorithm proposed in [49, 50] for CP-OFDM.

2.3.3 Channel Estimation

UA channels have the characteristics of long and fast time-varying multipath delay, thus estimating the channel is one of the technical

challenges. As UA channels vary significantly in different environments and is doubly selective in both time and frequency [11], channel estimation is a key factor for the UA communication system performance. Channel estimation can be performed based on pilot signals which is the mainstream method at present [70]. LS estimation and MMSE algorithm [51] are two major approaches for channel estimation. Then the interpolation method such as linear interpolation, time-frequency conversion interpolation can be used for channel estimation. In our research, the LS method is used followed by linear interpolation for channel estimation.

After Doppler effect estimation and compensation, ideally (11) can also be presented as

$$\begin{bmatrix} r_f[1] \\ r_f[2] \\ \vdots \\ r_f[K_s] \end{bmatrix} = \begin{bmatrix} S[1] & 0 & \dots & 0 \\ 0 & S[2] & & \vdots \\ \vdots & & \ddots & 0 \\ 0 & \dots & 0 & S[K_s] \end{bmatrix} \begin{bmatrix} h_f[1] \\ h_f[2] \\ \vdots \\ h_f[K_s] \end{bmatrix} + \begin{bmatrix} w_f[1] \\ w_f[2] \\ \vdots \\ w_f[K_s] \end{bmatrix} . \quad (14)$$

We index pilot subcarriers as the set $\mathcal{K}_p = \{p_1, \dots, p_{K_p}\}$ with $K_p := \overline{\mathcal{K}}_p$ subcarriers in total. Based on the input-output relationship in (14), arranging the frequency measurements at pilot subcarriers into a vector yields

$$\begin{bmatrix} r_{f_p}[1] \\ r_{f_p}[2] \\ \vdots \\ r_{f_p}[K_p] \end{bmatrix} = \begin{bmatrix} S_p[1] & 0 & \dots & 0 \\ 0 & S_p[2] & & \vdots \\ \vdots & & \ddots & 0 \\ 0 & \dots & 0 & S_p[K_p] \end{bmatrix} \begin{bmatrix} h_{f_p}[1] \\ h_{f_p}[2] \\ \vdots \\ h_{f_p}[K_p] \end{bmatrix} + \begin{bmatrix} w_{f_p}[1] \\ w_{f_p}[2] \\ \vdots \\ w_{f_p}[K_p] \end{bmatrix} . \quad (15)$$

Let us introduce $\boldsymbol{S}_p = diag(S_p[1], S_p[2], \dots S_p[K_p])$ and $\boldsymbol{r}_p$ as the received data in the pilot subcarriers in $\boldsymbol{r}_f$ which are equally spaced within the K_s subcarriers and known to the receiver. In order to recover the data $\widehat{\boldsymbol{S}}$, we

need to estimate the CFR $\widehat{\boldsymbol{h}}_{\boldsymbol{f}}$. The LS based channel estimation at pilot subcarriers is as follows [52, 71]

$$\begin{aligned}\widehat{\boldsymbol{h}}_{LS} &= \left(\boldsymbol{S}_p^H \boldsymbol{S}_p\right)^{-1} \left(\boldsymbol{S}_p^H \boldsymbol{r}_p\right) \\ &= \boldsymbol{S}_p{}^{-1} \boldsymbol{r}_p \end{aligned} \tag{16}$$

Then linear interpolation is applied to obtain the channel responses of the data subcarriers based on the channel responses at the pilot subcarriers.

2.3.4 SNR Estimation

Limited bandwidth, severe fading, strong multipath interference, significant Doppler shifts are the main limitations for UA communication. In addition to those challenges, UA noise has an impact on UA communication. UA noise consists of different components such as turbulence, wind-generated waves, rain, surface shipping and industrial activities, marine animals, ice cracking, snapping shrimp, earthquakes at the sea bed, oil and gas exploration and production etc. [25, 72].

Following the OFDM signal design, noise power and received signal power are estimated in the frequency domain at the receiver. In this research, the noise variance is estimated in null subcarriers and the received signal power is estimated in active (pilot and data) subcarriers. Received power at null subcarriers is estimated as

$$\hat{\sigma}_n^2 = \frac{1}{\bar{\mathcal{K}}_n} \sum_{n=1}^{\bar{\mathcal{K}}_n} \left| r_f[\mathcal{K}_n(n)] \right|^2 \tag{17}$$

where $\mathcal{K}_n$ is the set containing the indices of null subcarriers as the set $\mathcal{K}_n = \{n_1, \dots, n_{K_n}\}$ and for a set $\mathcal{X}$, $\bar{\mathcal{X}}$ denotes the number of elements in $\mathcal{X}$ and $r_f[n]$ is the frequency-domain received signal at the n th subcarrier.

Received power at active subcarriers is estimated as

$$\hat{\sigma}_a^2 = \frac{1}{\bar{\mathcal{K}}_a} \sum_{a=1}^{\bar{\mathcal{K}}_a} \left| r_f[\mathcal{K}_a(a)] \right|^2 \tag{18}$$

where $\mathcal{K}_a$ is the set containing the indices of pilot and data subcarriers i.e. $\mathcal{K}_a = \mathcal{K}_p \cup \mathcal{K}_d$ [25] as the set $\mathcal{K}_a = \{a, \dots, a_{K_a}\}$. $r_f[a]$ is the frequency-domain received signal at the a th subcarrier. Then the SNR in the frequency domain can be estimated as

$$\bar{\gamma} = \frac{\hat{\sigma}_a^2}{\hat{\sigma}_n^2} - 1 \tag{19}$$

.

Chapter 3

Frame-Based Adaptive Modulation

Limited bandwidth and time-varying multipath propagation place significant constraints on the achievable throughput of UA communication systems. So, OFDM adaptive modulation schemes have been introduced to increase the bandwidth efficiency and data rate of the UA systems. In this chapter, a frame-based adaptive modulation scheme is proposed which ensures higher data rate and better spectral efficiency of the UA communication systems. Simulation and experimental results are presented to demonstrate the effectiveness of the proposed frame-based adaptive scheme.

3.1 Introduction

Most applications require a certain minimal BER and an adaptive modulation scheme can be designed to have a BER which is constant for all channel SNR. In general, the spectral efficiency of the non-adaptive modulation is constant whereas in adaptive schemes, spectral efficiency increases with the increase of channel SNR. Thus, by using adaptive modulation schemes, the spectral efficiency can be improved and

simultaneously a better suited BER is possible according to the requirement of application. This is the reason that adaptive schemes become much more effective for data transmission [73].

In adaptive OFDM modulation, each subcarrier can be independently modulated or all subcarriers can be modulated in the same manner [58]. In this research, frame-based and cluster-based adaptive modulation schemes have been developed where the adaptation is done frame by frame. In the frame-based adaptive scheme, all subcarriers of one frame are modulated with one modulation size and in the cluster-based adaptive scheme, group of subcarriers (clusters) of one frame are modulated with different modulation sizes.

In the proposed frame-based adaptive scheme, the SNR of each received data frame is estimated at the receiver and used as CSI to choose the adaptive allocation of the transmission parameters. The receiver then sends this information back to the transmitter for the next data frame. In this scheme, different modulation constellations (size) are selected based on the received SNR for the next data frame and the highest order modulation can be chosen depending on the channel conditions. Higher order modulations enables the transmission of more bits per symbol and thus higher data rate and better spectral efficiency can be achieved. Compared with cluster-based adaptive modulation, the frame-based adaptive modulation requires less amount of CSI feedback as only one modulation size needs to be fed back for each frame for the next transmission.

3.2 Adaptive Allocation of Transmission Parameters

In this chapter, frame-based adaptive OFDM is discussed where modulation size is adaptively allocated for the transmission. The block diagram of the proposed adaptive modulation scheme in Figure 6 shows that the frequency offset estimation and compensation are done at the receiver side. Then channel estimation and SNR estimation are performed. Then modulation modes are selected by the mode selector block depending on the estimated received SNR for the next data frame. The selected modulation mode for the next data frame is fed back to the transmitter.

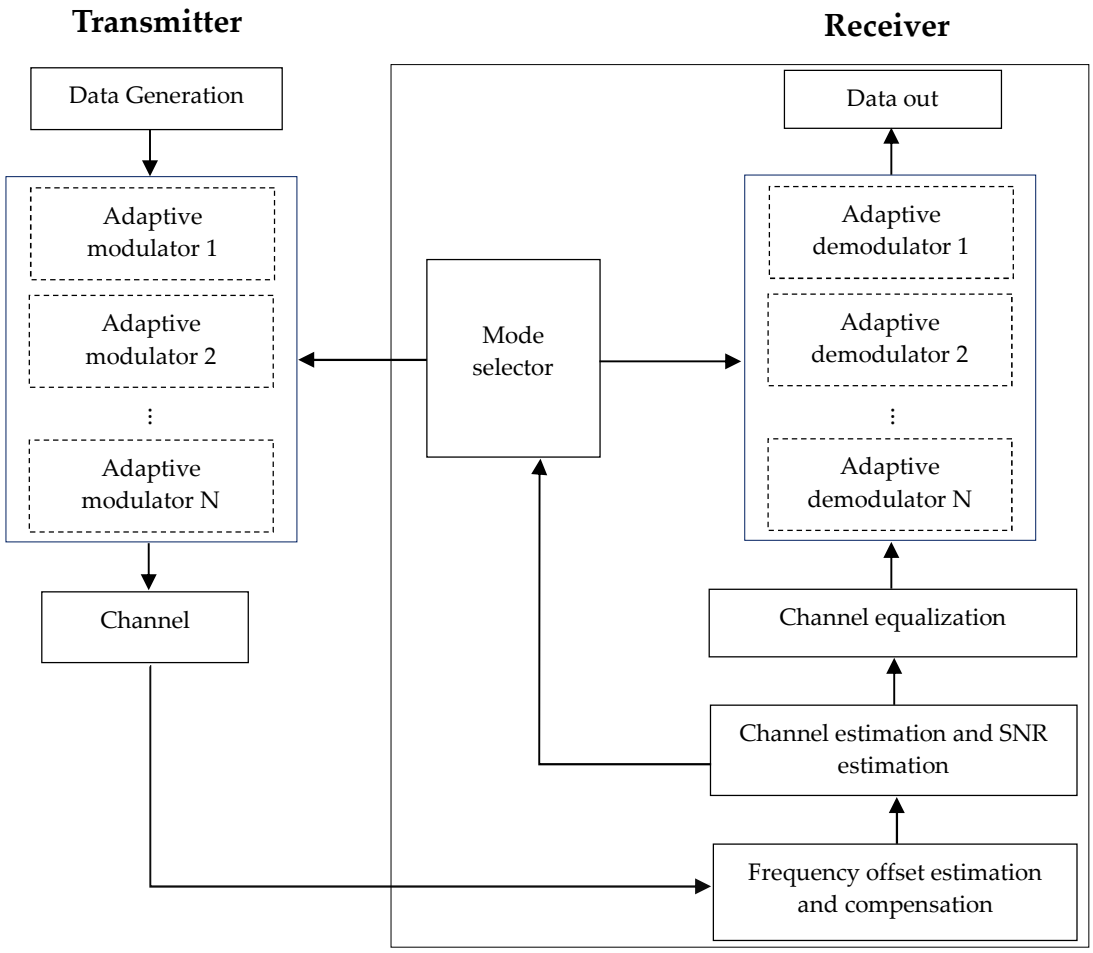

Figure 6: Block diagram of the adaptive modulation scheme.

The adaptive modulator block at the transmitter side consists of different modulators which provide different modulation mode and modulate the data frame according to the selected mode. The demodulator block demodulates the received signal according to the selected modulation mode. For the frame-based adaptive scheme, the effect of Doppler frequency in adaptive modulation is also studied. Adaptive modulation becomes challenging with the increase of Doppler frequency which leads to significant ICI. ICI deteriorates the system performance as it enhances the power of received signal in the inactive (null) subcarriers and also misleads the detection of transmitted signal on active subcarriers. Thus the ICI affects the estimation of the received SNR, which in turn affects the performance of adaptive modulation.

We show in this chapter that, the proposed frame-based adaptive modulation scheme increases the data rate of UA communication systems and performs better for lower Doppler frequency i.e. for slowly moving transmitter and/or receiver. For rapidly moving transmitter and/or receiver, the ICI becomes more prominent. In the presence of ICI, the estimated noise power is not only due to the actual noise but also due to ICI which affects the SNR estimation. As the adaptive allocation of modulation size depends on the SNR estimation, the performance of the proposed adaptive modulation scheme deteriorates for higher Doppler frequency which means the adaptive UA OFDM communication system becomes limited by interference rather than by noise.

3.3 System Implementation

A combination of NI LabVIEW software and CompactDAQ device are adopted for real-time adaptive modulation for UA OFDM communication

systems. The system design including both the transmitter and receiver is discussed. An implementation of OFDM-based modems for UA communication using the TMS320C6713 DSP development board has been demonstrated in [34]. However, such DSP-based implementation can be time consuming on system design and development. The NI CompactDAQ device combined with the LabVIEW software provide an attractive solution to simplify the prototype design and reduce the software development time. NI CompactDAQ is a robust and reliable measurement system, capable of working with a series of NI I/O modules. LabVIEW is a graphical programming language which simplifies hardware integration so that one can rapidly acquire and visualize data sets from NI or third-party I/O device virtually, resulting in a reduced programming and debugging time [39, 40]. The performance of the real-time frame-based adaptive OFDM system is verified through a UA communication experiment conducted in a tank.

3.3.1 System Hardware

An NI CompactDAQ system is used for signal generation and acquisition in our UA OFDM communication system. CompactDAQ is capable of analog I/O, digital I/O, counter/timer operations, and industrial bus communication. The following system hardware are used in the frame-based adaptive UA OFDM system.

- NI cDAQ-9174 – transfer data between computer and I/O devices.
- NI-9260 – output signals to the transducer.
- NI-9232 – acquire signals from the hydrophone.
- CTG0052 – transmitter transducer.
- Reson Reference TC 4034 – receiver hydrophone.

- HTI-96-Min - receiver hydrophone.

The CompactDAQ system which we use in our system design consists of a chassis and two NI I/O modules as described in the following section.

3.3.1.1 NI cDAQ-9174 Chassis

In the CompactDAQ system, an NI cDAQ-9174 chassis is a plug-and-play chassis designed for small portable sensor measurement systems. It controls the timing, synchronization, and data transfer among up to four I/O modules and an external host (e.g. desktop computer) via a USB cable. A mix of digital I/O, analog I/O, and counter/timer measurements can be created with this chassis. The cDAQ-9174 also has four 32-bit general purpose counters/timers. Using multiple timing engines, up to seven hardware-timed operations can be conducted simultaneously, with three independent rates for analog input.

3.3.1.2 NI-9260

NI-9260 is a two-channel voltage output module. It features a 51.2k samples/s update rate, 24-bit resolution, 3 V output range, and ±30V over-voltage protection. In the proposed adaptive UA OFDM system, this module is plugged into the cDAQ-9174 chassis to transmit signals to the transducer.

3.3.1.3 NI-9232

The NI-9232 is a 3-channel dynamic signal acquisition module with a maximum sampling rate of 102.4k sample/second/channel. These three input channels can perform signal measurement simultaneously and each channel has built-in anti-aliasing filters that automatically adjusts to its sample rate. Together with NI software, the NI-9232 module can execute signal processing functions, such as order tracking and frequency analysis of the

received signal. In the proposed adaptive UA OFDM system, this module is plugged into the cDAQ-9174 chassis to acquire signals received from the hydrophone.

3.3.1.4 CTG0052

The CTG0052 UA transducer from Chelsea Technologies is a high power and low frequency transducer. The effective frequency range of this transducer is 8–16 kHz, which covers the spectrum of telephony, telemetry, and other UA applications. In the proposed system design, the transducer is connected to the NI-9260 module through a transformer matching network and a power amplifier to transmit acoustic signals through the underwater channel.

3.3.1.5 HTI-96-Min

The HTI-96-Min portable hydrophone from High Tech Inc., Long Beach, MS, USA, is widely applied in UA communication systems. The sensitivity of this hydrophone is −201 dB re: 1 V/μPa with a frequency range of 2 Hz–30 kHz. In the proposed adaptive UA OFDM system, this hydrophone is connected to the NI-9232 module through a preamplifier to acquire signals received from the UA channel.

3.3.1.6 Reson Reference TC 4034

The TC4034 broadband spherical hydrophone provides uniform omnidirectional characteristics over a wide frequency range of 1Hz to 480 kHz with receiving sensitivity -218dB ±3dB (re 1V/μPa). In the proposed system design, this hydrophone is connected to the NI-9232 module through a preamplifier to acquire signals received from the UA channel.

In the system design of the proposed frame-based adaptive modulation scheme, an NI cDAQ-9174 plug-and-play chassis is connected to a laptop through USB where the NI LabVIEW software is installed for the signal generation, acquisition and processing. An NI-9260 and an NI-9232 are plugged into two of the four slots of the chassis for signal generation and acquisition respectively. The CTG0052 acoustic transducer is connected to the NI-9260 module through a transformer matching network and a power amplifier to transmit acoustic signals through the UA channel. The Reson reference hydrophone (forward link) and HTI-96-Min hydrophone (feedback link) are connected to the NI-9232 modules through preamplifiers to acquire signals received from the UA channel for the forward and feedback links respectively. For adaptive modulation two sets of devices are used. One set is designed for the forward link and the other set is designed for the feedback link.

3.3.2 Software Implementation

The software of the proposed frame-based adaptive UA OFDM system is designed and implemented using NI LabVIEW. The system generates one frame and forwards the generated data frame to the channel 1 of NI 9260 (DAQ1/Slot2/channel1). The transducer (a) transmits the signal through the UA channel. Then the hydrophone (a) receives the signal and forwards the received data to NI9232 (DAQ2/Slot1/channel1). Then the signal is processed by the receiver in LabVIEW. At first, the signal samples received by NI9232 are converted from the passband to the baseband. The receiver first removes the CP from each OFDM block. Then the frequency offset estimation and compensation is performed for each OFDM symbol using the null subcarriers. Then the SNR is estimated in the frequency domain. After that

the baseband signals are passed through channel estimation. The LS method is used to estimate the frequency domain channel response at the pilot subcarriers. The estimated channel response is used to equalize the received signals. Demodulation operation is performed to the equalized signals.

After estimating the SNR of the received signal, the modulation size is selected depending on the channel condition for the next frame transmission. For performing the adaptive modulation scheme, data symbols containing the adaptively selected transmission parameters information are modulated by QPSK constellations at the feedback transmitter in LabVIEW. Then the data frame is forwarded to the channel 1 of the data generation module NI-9260 (DAQ2/Slot2/channel 1) of the feedback link. The feedback channel operates in time-division duplexing (TDD). There is a guard time to process the received signal before sending the feedback signal. The transducer (b) feeds back the modulation size information signal through the UA feedback channel. The hydrophone (b) receives the modulation size signal and forwards the received data to NI9232 (DAQ1/Slot1/channel1) for processing. The real-time adaptive modulation scheme is shown in Figure 7 where transducer (a) and transducer (b) refer to the CTG0052 transducer, hydrophone (a) refers to the Reson reference hydrophone and hydrophone (b) refers to HTI-96-Min hydrophone.

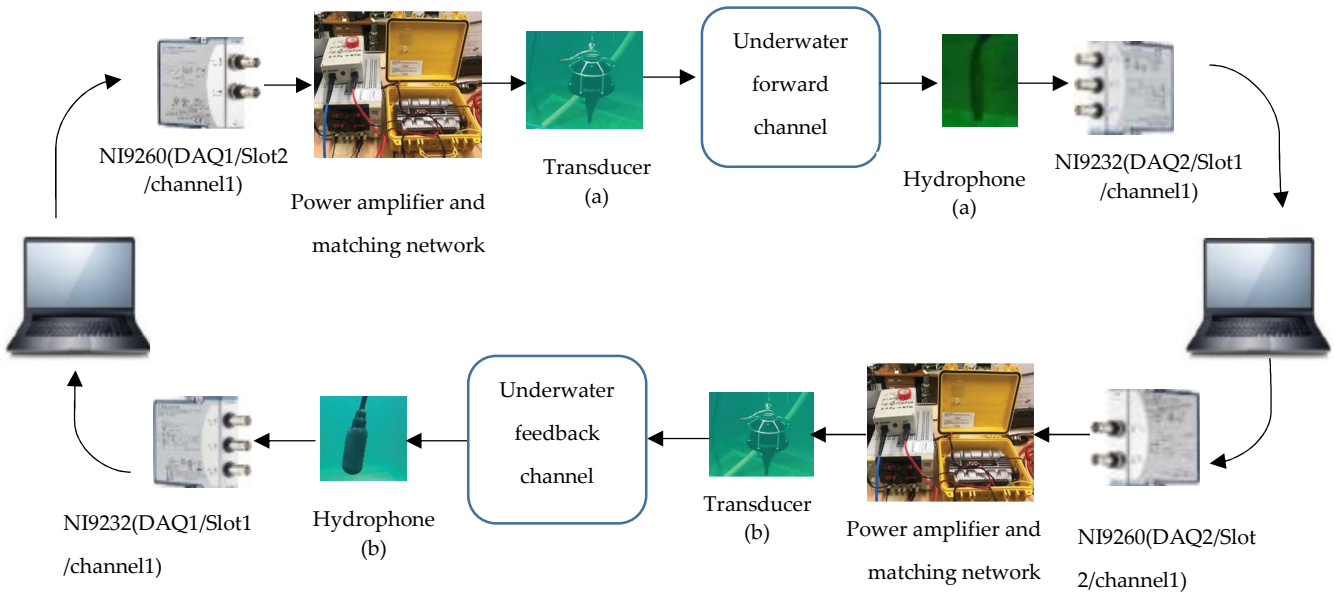

Figure 7: LabVIEW-based implementation of real-time adaptive modulation for UA OFDM system.

3.4 Results and Discussions

In this section, the simulation and experimental results of the frame-based adaptive modulation scheme are presented and discussed.

3.4.1 Simulation Results

UA channels are generally characterized by randomly time-varying multipath propagation which results in frequency selective fading [35]. Additionally, motion of the transmitter and/or receiver introduces Doppler shift to the channel which contributes to the changes in CIR. In simulation a multipath Rayleigh fading channel is generated. The parameters used to generate the Rayleigh channel are listed in Table 1. The UA channel is simulated with 5 paths. The paths are correlated and the arrival times of all paths follow a Poisson distribution with an average delay of 1 ms between two adjacent paths. The moving speed corresponds to the Doppler frequency

and same for all paths. When the moving speed is 0.001 m/s, the corresponding Doppler frequency is 0.0139 Hz. The amplitudes of the paths are Rayleigh distributed with variances following an exponentially decreasing profile.

Table 1: Parameters used in simulation to generate the channel.

Number of path	5
Delay mean	10^{-3} s
Move speed	0.001 m/s
Sound speed	1500 m/s
Exponentially decreasing factor for generating amplitude profile	-1000.2

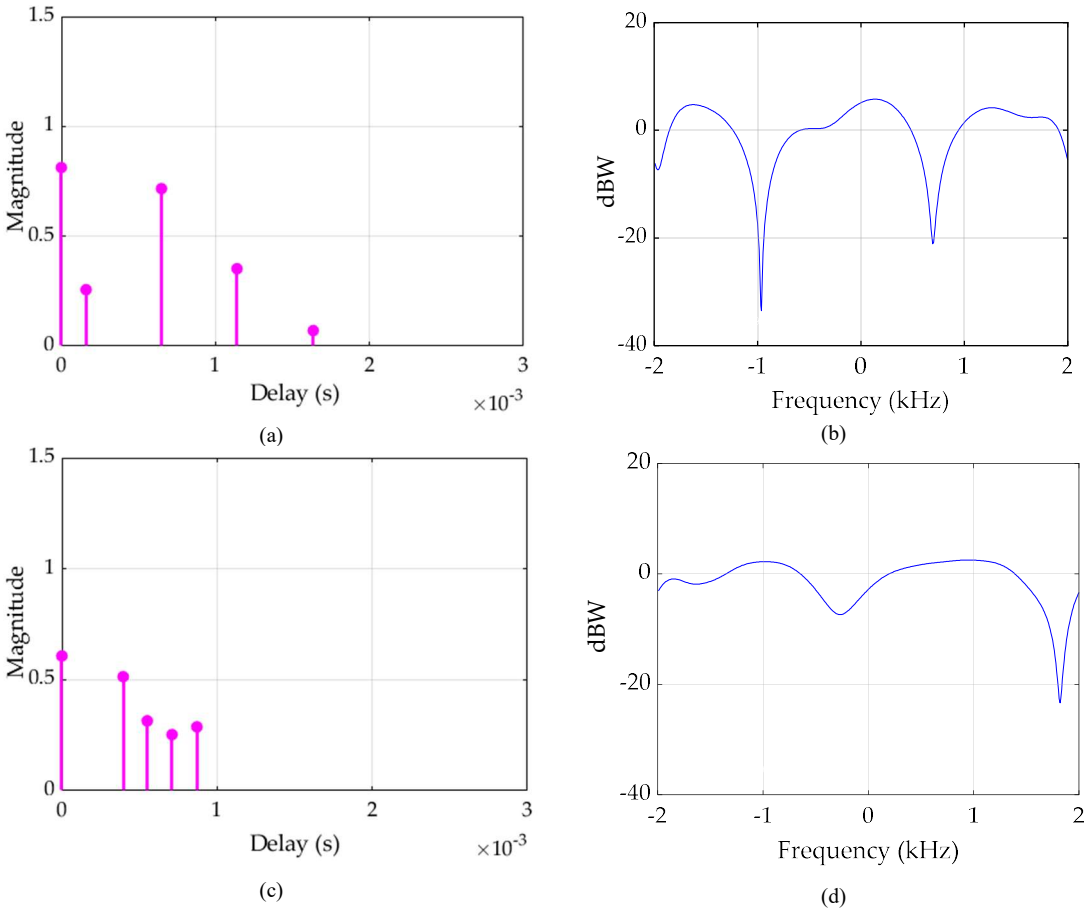

Figure 8: CIRs and CFRs of the UA channel for the first OFDM frame (a and b) and the fifth OFDM frame (c and d).

Figure 8 depicts the simulation results of the time-varying CIRs and CFRs of the first and fifth OFDM frames. At each path, the channel gain is Rayleigh distributed. From Figure 8 (a) and 8 (c), it is observed that there are five paths in the channel, and the arrival time (delay (s)) of the five paths are different between the first and the fifth OFDM frames. It is also seen that the magnitude of CIRs is varying fast between the first and the fifth frame. In Figure 8 (a) and 8 (c), both the arrival time and magnitude of the paths are varying, which illustrate the time-varying characteristics of the multipath channel. Figure 8 (b) and 8 (d) show the frequency response of the channel. The frequency selective fading is also observed from Figure 8 (b) and 8 (d) as the power level (dbW) varies over the signal bandwidth.

In the frame-based adaptive modulation scheme, individual modulation scheme results have been observed and analyzed for UA communication systems with fixed modulation. Extensive simulations of fixed modulation for different modulation schemes are used to select the target BER and the estimated SNR is used as switching parameter [46, 74]. Switching thresholds for adaptive modulation system are determined to keep the overall BER lower than the target BER. In fact, the highest modulation order is chosen under a certain BER and SNR. Therefore, a better tradeoff between data rate and overall BER is achieved by the proposed adaptation system.

In this research, the performance of the proposed adaptive modulation relies on the accuracy of the SNR estimation, as the received SNR is determined as switching parameter. The estimated SNR needs to be as close as possible to the actual SNR. The SNR is estimated after the CFO estimation and compensation which is shown in Figure 6. At lower Doppler frequency, the SNR estimation algorithm can estimate the SNR nearly close to the actual

SNR. However, at higher Doppler frequency, the SNR is not estimated close to actual SNR as the estimated noise power increases due to ICI. Figure 9 shows the estimated SNR for different Doppler frequencies for fixed modulation. The estimated SNRs for lower Doppler frequency of 0.0139 Hz and 0.1386 Hz are depicted by the diagonal upward straight line, which indicates that the estimated SNR is close to the actual SNR at lower Doppler frequency. However, at higher Doppler frequency of 1.3856 Hz, the SNR is estimated close to the actual SNR up to 15 dB, then the diagonal straight line starts to bend downward when SNR reaches above 15 dB. Therefore, it can be said that adaptive modulation performs well around the lower SNR range (<15 dB) at higher Doppler frequency.

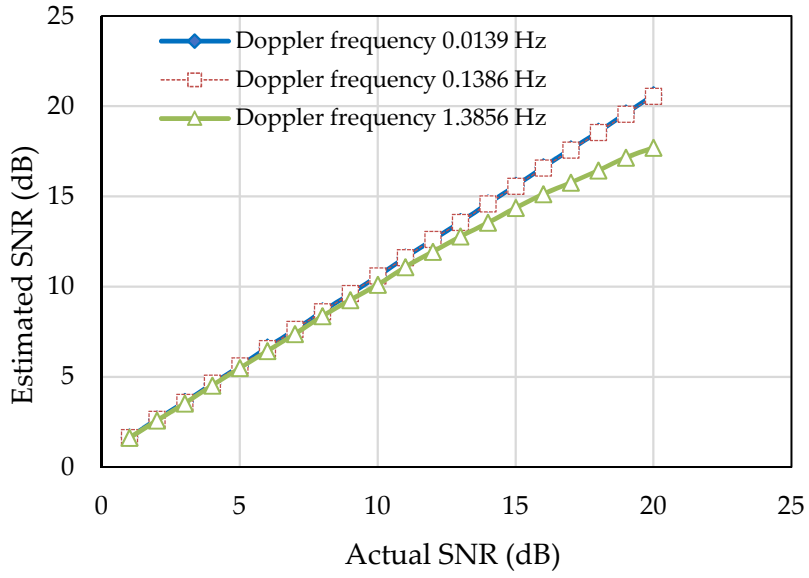

Figure 9: Estimated SNR for different Doppler frequencies for fixed modulation.

For simulation, 512 subcarriers are considered in each block of the UA OFDM system and five paths are considered in the UA channel. Maximum Doppler shift varies from 0.0139 Hz to 1.3856 Hz. The system parameters used in the simulation are listed in Table 2.

Table 2: Parameters used in simulation of frame-based adaptive scheme.

Bandwidth	B = 4 kHz
Number of subcarriers	K_s = 512
Subcarrier spacing	f_{sc} = 7.8 Hz
Length of OFDM symbol	T = 128 ms
Length of CP	T_{cp} = 25 ms
Preamble size	N_{pn} = 510
Number of pilot subcarriers	K_p = 128
Number of data subcarriers	K_d = 320
Number of null subcarriers	K_n = 64

At first, the BER performance of the fixed modulation using BPSK, QPSK, and 16QAM constellations are studied. Then, after investigating the SNR versus BER results of the fixed modulation, the target BER and switching thresholds are determined. Figure 10 shows the BER performance of adaptive modulation and fixed modulation system for different Doppler frequencies. It is seen that, for the lower Doppler frequency (0.0139 Hz and 0.1386 Hz), the target BER is selected as low as 0.01. On the other hand, for higher Doppler frequency (1.3856 Hz), the selected target BER is 0.1. Switching thresholds used in the simulation for the frame-based adaptive modulation schemes are presented in Table 3, Table 4 and Table 5 for Doppler frequencies of 0.0139 Hz, 0.1386 Hz, and 1.3856 Hz. The target BER is higher for higher Doppler frequency compared to lower Doppler frequency, as Doppler frequency-induced ICI places a limit on the SNR estimation at higher SNR range. Therefore, it can be said that in the presence of ICI, not only the actual noise power but also the ICI is reflected in the

estimated noise power which affects the SNR estimation. This means that the performance of the proposed adaptive modulation scheme becomes limited not only by noise but also interference at higher Doppler frequency.

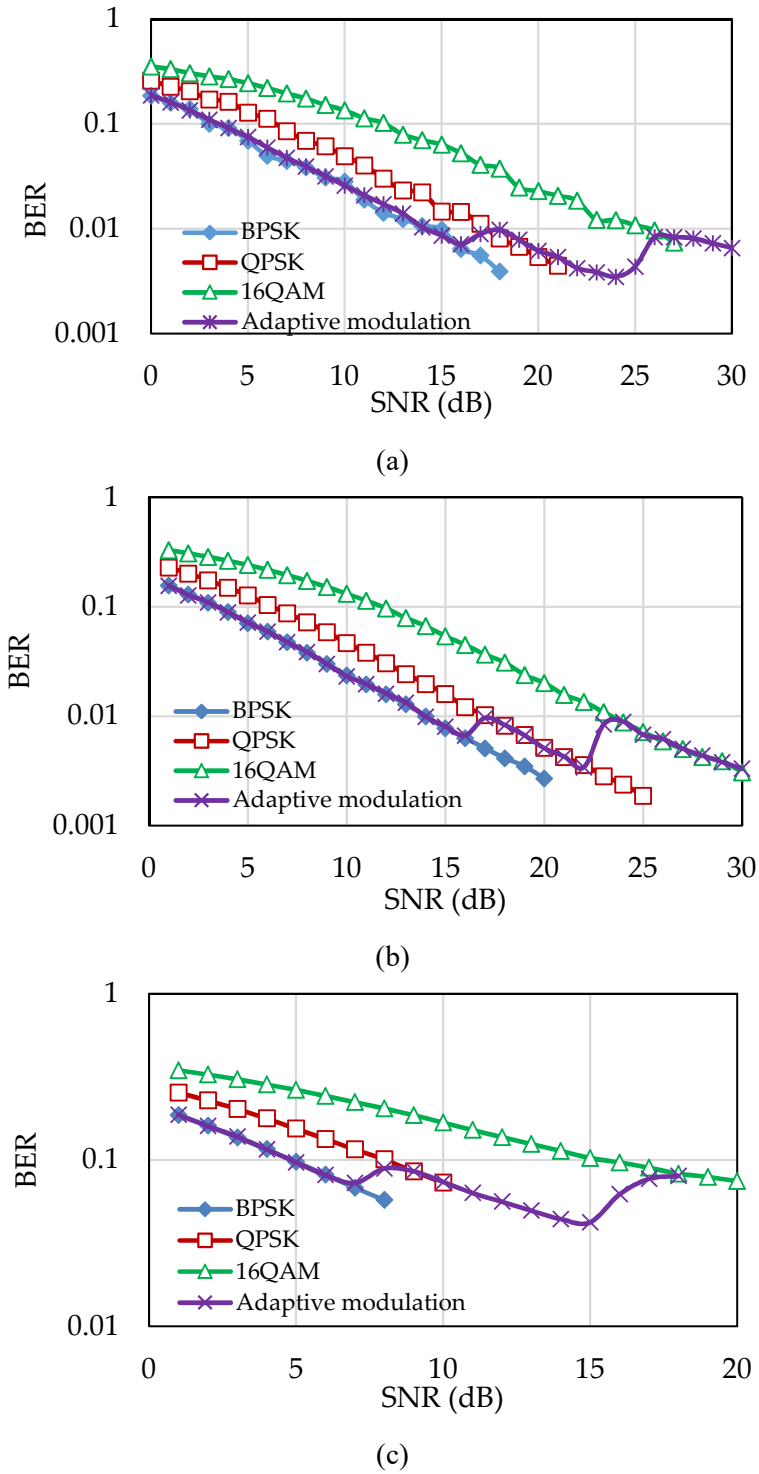

Figure 10: BER performance of the proposed adaptive modulation scheme for Doppler frequency (a) 0.0139 Hz, (b) 0.1386 Hz and (c) 1.3856 Hz.

Table 3: Switching threshold for frame-based adaptive modulation scheme at target BER 0.01 for Doppler frequency 0.0139 Hz

Mode	Modulation	Threshold
1	BPSK	SNR < 17.35 dB
2	QPSK	17.35 dB ≤ SNR ≤ 25.7 dB
3	16QAM	SNR > 25.7 dB

Table 4: Switching threshold for frame-based adaptive modulation scheme at target BER 0.01 for Doppler frequency 0.1386 Hz

Mode	Modulation	Threshold
1	BPSK	SNR < 17.1 dB
2	QPSK	17.1 dB ≤ SNR ≤ 23.4 dB
3	16QAM	SNR > 23.4 dB

Table 5: Switching threshold for frame-based adaptive modulation scheme at target BER 0.1 for Doppler frequency 1.3856 Hz

Mode	Modulation	Threshold
1	BPSK	SNR < 8 dB
2	QPSK	8 dB ≤ SNR ≤ 15.4 dB
3	16QAM	SNR > 15.4 dB

From Figure 5, it can be seen that each frame contains five OFDM data blocks and one preamble block. In simulation, the preamble block contains $K_{pre} = 510$ subcarriers. In data blocks, among the total 512 subcarriers, there are 320 data subcarriers, 128 uniformly spaced pilot subcarriers and 64 null subcarriers. The number of information-carrying uncoded bits in each frame is $K_b = 1600$ for BPSK, $K_b = 3200$ for QPSK, $K_b = 6400$ for 16QAM. The data rate of the fixed modulation system is estimated as

$$D_r = \frac{K_b}{T_{fr}} \tag{20}$$

where frame duration, $T_{fr} = \left(\left(T + T_{cp}\right) K_{blk}\right) + T_{pre}$ and T_{pre} is the preamble duration.

The data rate of fixed modulation is fixed for each transmission. In this simulation the data rates of BPSK, QPSK and 16QAM are 1.79 kbps, 3.59 kbps and 7.17 kbps respectively. Alternatively, the data rate of adaptive modulation changes in each transmission depending on the estimated received SNR. The data rate of the fixed modulation and the adaptive modulation is shown in Figure 11. It can be seen that the data rate of the fixed modulation is constant at any channel condition whereas the data rate of the adaptive modulation changes according to the channel conditions. From the simulation results, it can be said that no fixed OFDM system can provide a better BER performance while simultaneously providing a better data rate. The proposed adaptive system can ensure a higher data rate at the target BER compared with the fixed modulation.

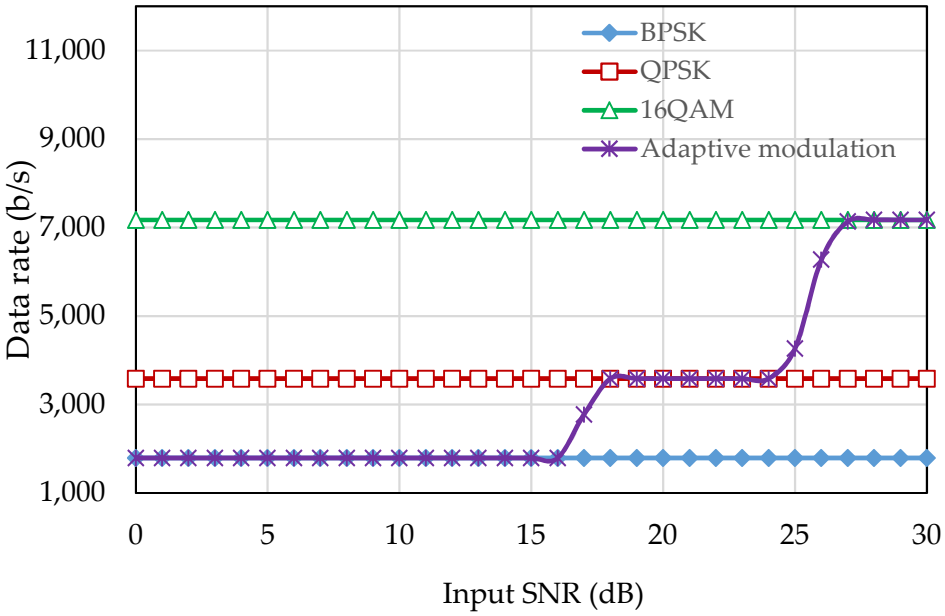

Figure 11: Data rate of the frame-based adaptive modulation.

Table 6: Parameters used in the tank experiment of the frame-based adaptive modulation scheme.

Bandwidth	B = 4 kHz
Number of subcarriers	K_s = 512
Subcarrier spacing	f_{sc} = 7.8 Hz
Length of OFDM symbol	T = 128 ms
Length of CP	T_{cp} = 25 ms
Number of pilot subcarriers	K_p = 128
Number of data subcarriers	K_d = 325
Number of null subcarriers	K_n = 59

3.4.2 Experimental Results

In the tank experiment, in order to obtain the switching SNR thresholds for various modulation schemes under a target BER, we first perform one-way communication experiment with a pair of transducer and hydrophone. The received SNR is changed through varying the power of the transmitted signal. The system parameters used in the tank experiment are listed in Table 6. Switching thresholds that obtained from the fixed modulation experiment are listed in Table 7.

Table 7: Switching threshold for the frame-based adaptive modulation scheme at target BER 0.1 in the tank experiment.

Mode	Modulation	Threshold
1	BPSK	SNR < 13.25 dB
2	QPSK	13.25 dB ≤ SNR ≤ 24.5 dB
3	16QAM	SNR > 24.5 dB

After obtaining the SNR thresholds, the experiment of adaptive modulation is performed by placing another pair of transducer and hydrophone in the tank. Figure 12 shows the location of the transducers and hydrophones in the tank during the experiment. The length, width and depth of the tank are 2.5 m, 1.5m and 1.8 m respectively. During the tank experiment, we bypassed the frequency offset estimation and compensation module in Figure 6 as the Doppler shift is very small in a tank.

Figure 12: Location of the transducers and hydrophones for forward and feedback links.

The block diagram of the receiver operation and one successfully detected data frame and magnitude of the cross-correlation between the received synchronization sequence and local synchronization sequence are shown in Figure 13. The waveforms in the figure are shown as the output of the corresponding blocks. The peak position represents the position of the strongest channel path while other non-negligible local peak values represent the other channel path positions which means that there are multiple paths between the transmitter and receiver because of the reflections of acoustic signals in the wall of the tank. The cross-correlation of the CIR estimated by the pilot subcarriers is shown in Figure 14. It can be seen that the maximum channel delay spread is 15 ms which is shorter than the CP length.

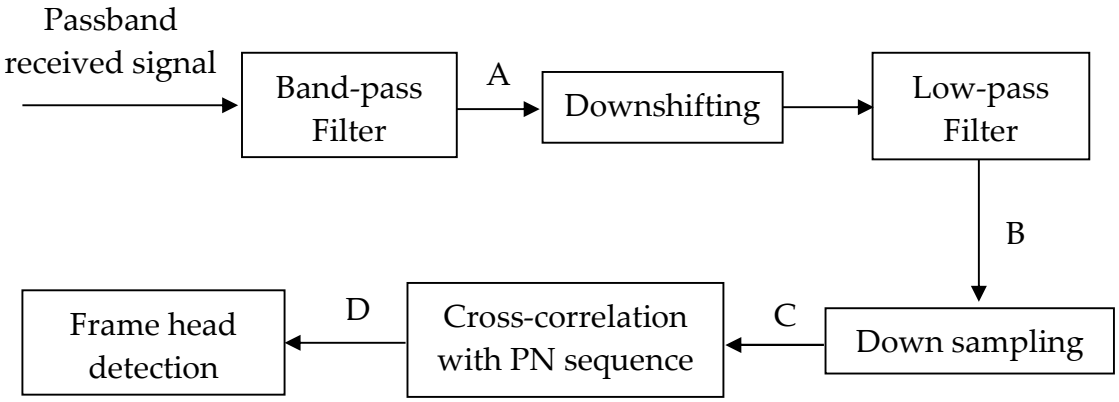

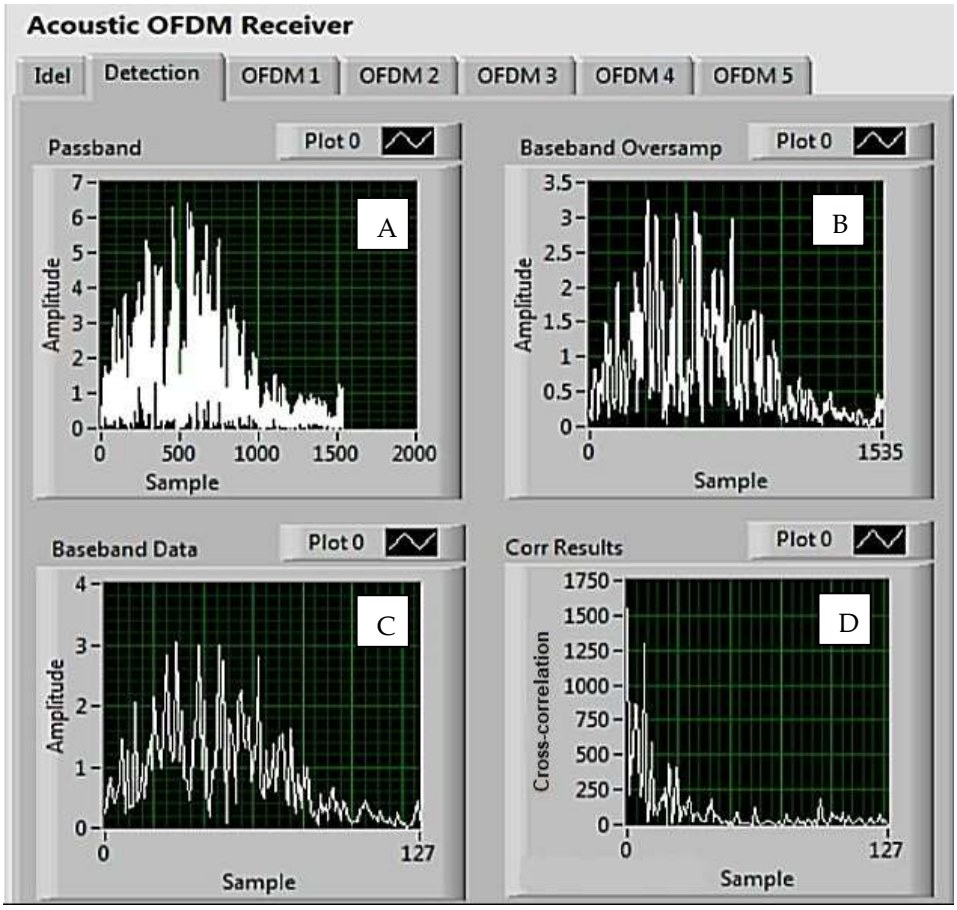

Figure 13: Received data frame in acoustic OFDM receiver is shown with the corresponding block diagram of the receiver operation during the tank experiment of the frame-based adaptive modulation scheme.

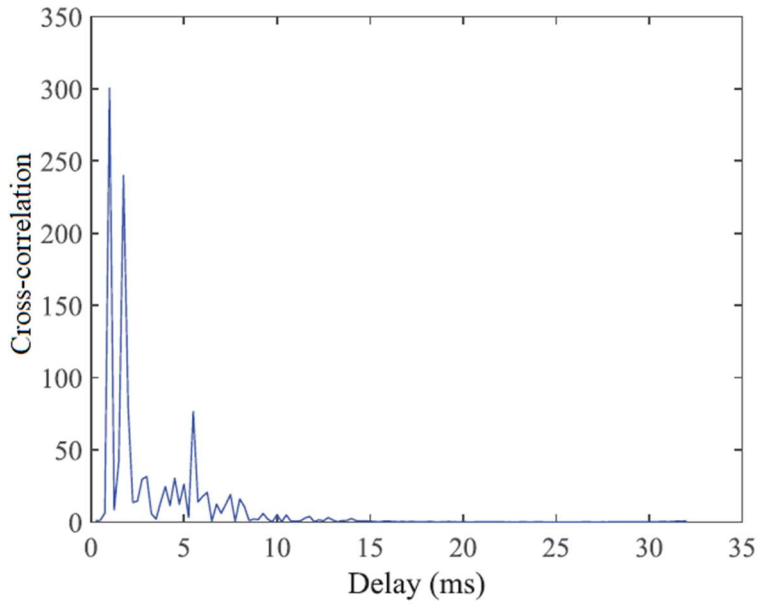

Figure 14: Cross-correlation of the CIR during the tank experiment of the frame-based adaptive modulation scheme.

Figure 15 shows the LabVIEW interface of the frame-based adaptive modulation for UA OFDM system performed in the tank. The first OFDM frame transmits with the BPSK constellations (indicated by "1" in the top ModSize box in Figure 15 (a)) and the received symbols are correctly aggregated into the BPSK constellations after the channel equalization.

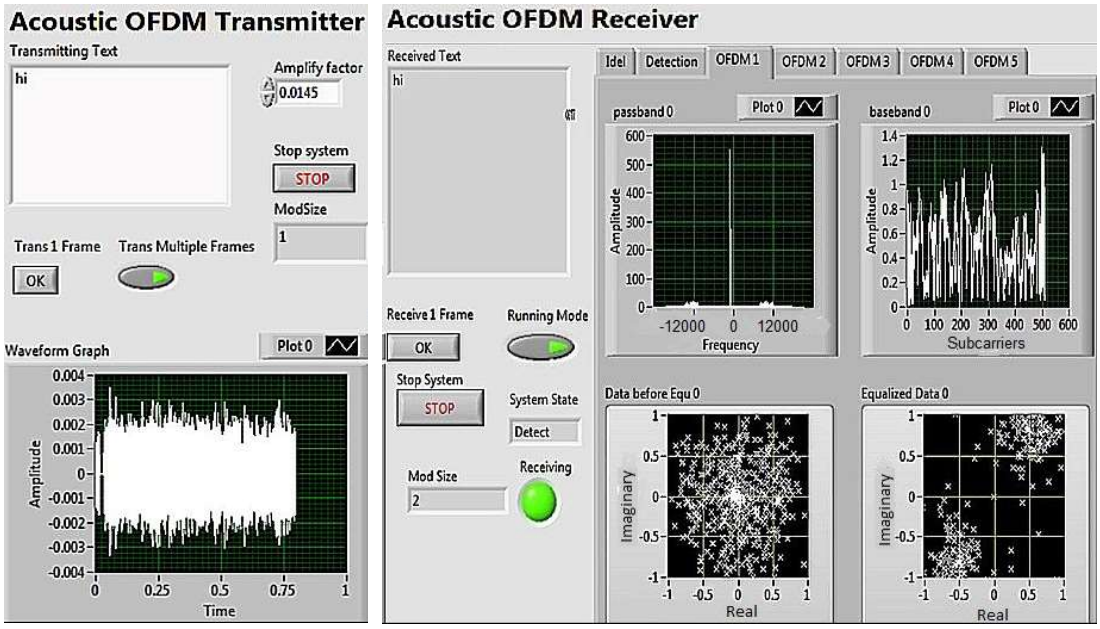

(a) (b)

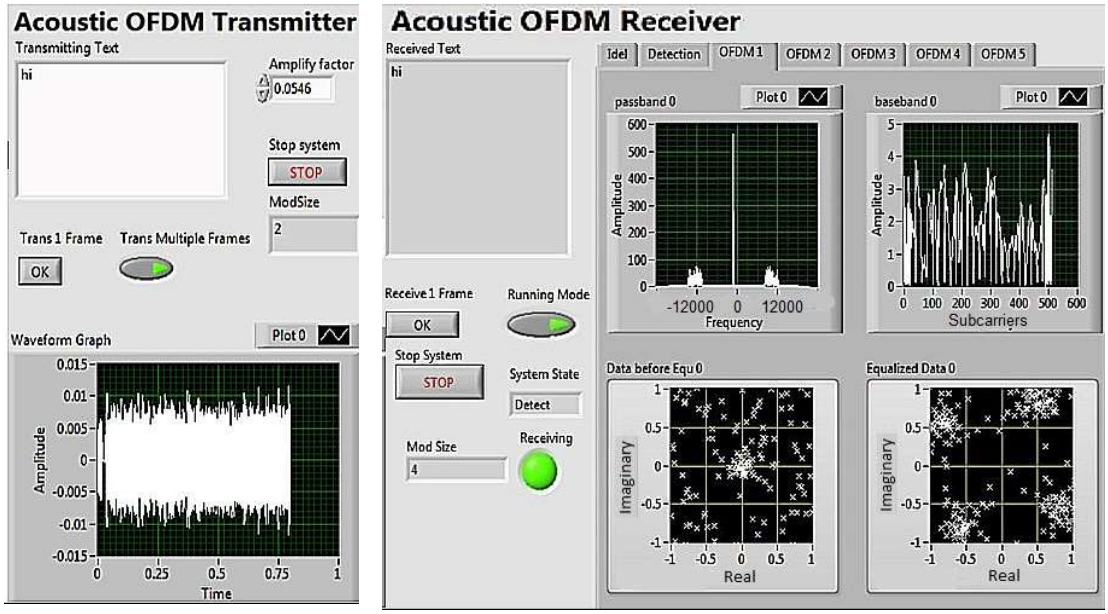

(c) (d)

Figure 15: Frame-Based adaptive modulation for UA OFDM system in the tank experiment.

As the received SNR is within the thresholds of the QPSK modulation in Table 7, the modulation size is selected to QPSK (as indicated by "2" in the lower Mod Size box in Figure 15 (b)) in the receiver side and fed back to the transmitter for the next transmission. Then the next OFDM frame transmits with the QPSK constellations (indicated by "2" in the top ModSize box in Figure 15 (c)) and the received symbols of the next frame are correctly aggregated into the QPSK constellations. As we further increase the transmit signal power, the received SNR is above the threshold of the 16QAM modulation in Table 7. Thus, the receiver feeds back this modulation scheme (indicated by "4" in the lower Mod Size box in Figure 15 (d)).

The BER vs SNR results are shown in Fig. 16 for fixed (BPSK, QPSK and 16QAM) and adaptive modulation schemes. The target uncoded BER in this experiment is determined as 0.1. Switching thresholds for the frame-based adaptive modulation scheme are determined using the BER results of the

fixed modulation schemes in Figure 16 and presented in Table 7 to keep the overall BER lower than 0.1. Thus, a better tradeoff between data rate and overall BER can be achieved by the proposed adaptation system.

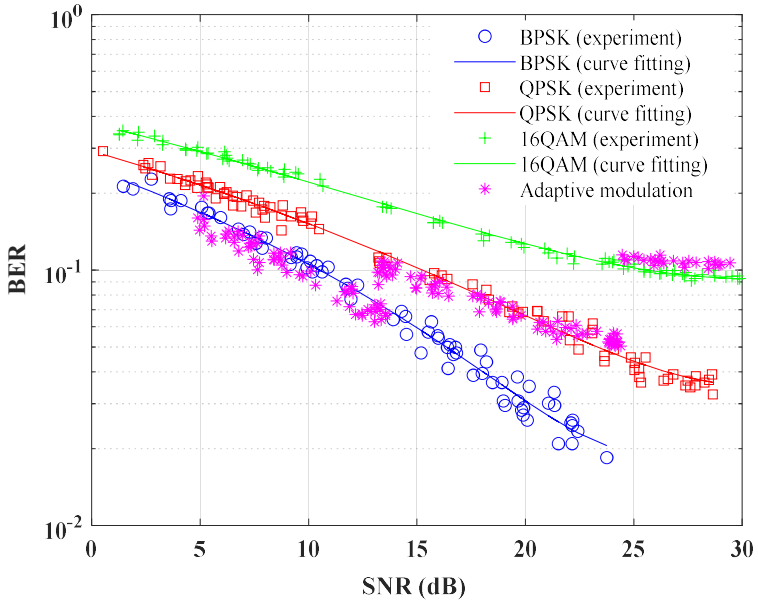

Figure 16: BER performance of the proposed adaptive modulation schemes in tank experiment.

3.5 Conclusion

A frame-based adaptive modulation scheme is presented in this chapter with simulation and experimental results. This adaptive modulation scheme is also studied for different Doppler frequencies. For higher Doppler frequency, the performance of adaptive modulation becomes challenging due to the ICI which affects the SNR estimation. Received SNR is chosen as performance metric for mode switching which also reflects the effect of ICI. The adaptive scheme depends on the estimated received SNR of the previous frame to choose adaptive allocation of the modulation size for the next frame transmission.

Extensive fixed modulation is investigated with different modulation schemes in OFDM system to choose the target BER to perform the adaptive modulation. The simulation results and the performance results of the real-time tank experiment prove that the highest modulation size is chosen under certain BER and SNR. Therefore, a better tradeoff between data rate and overall BER is achieved. Moreover, the proposed frame-based adaptive system can ensure higher data rate at the target BER compared to fixed modulation. In the frame-based adaptive modulation scheme, all subcarriers are modulated in the same manner. Hence, it requires low feedback rate, which makes it more robust.

Chapter 4

Cluster-Based Adaptive Modulation

UA channel is time-varying and some subcarriers of the OFDM system may be subject to a deep fading. To mitigate this effect subcarrier-based adaptive modulation scheme is chosen where each subcarrier or group of subcarriers (i.e. cluster) can be modulated independently. In this research, cluster-based adaptive modulation is selected to reduce the computational complexity and feedback load of the adaptive scheme. SNR is estimated at the receiver for each group of subcarriers i.e. cluster. The received cluster SNR is used as the CSI to choose the adaptive allocation of the transmission parameters for each cluster, which are sent back to the transmitter for the next data frame. In the cluster-based adaptive scheme, modulation size, subcarriers and transmit power are adaptively allocated for the transmission. The cluster-based adaptive modulation scheme ensures high data rate, improved energy efficiency and an overall better throughput of the UA OFDM system.

4.1 Introduction

In this research, OFDM and adaptive modulation and coding technique is considered in order to achieve high spectral efficiency, improve the

reliability of communication, improve the energy efficiency and boost the data rate. In the adaptive OFDM modulation, each subcarrier can be independently modulated or all subcarriers can be modulated in same manner [58]. As UA channel is fast varying and some subcarriers experience deep fading according to environmental conditions, subcarrier-based adaptive scheme is studied. Subcarrier-based adaptive scheme allows the system to discard the deep faded (i.e. weak) subcarriers for the next transmission and modulate the remaining subcarriers independently with different modulation sizes according to the CSI. This scheme also allows to distribute the residual power which is wasted for transmitting weak subcarriers among the remaining subcarriers for next transmission.

In the proposed frame-based adaptive modulation scheme, all subcarriers of an OFDM frame are modulated in same manner. Hence, one modulation size is fed back from the receiver to transmitter for the next frame. If each subcarrier of an OFDM frame is modulated independently, the computational complexity and feedback load for the adaptive scheme will be very high as the modulation size of each subcarrier needs to be fed back. This is why, the subcarriers of an OFDM frame are divided into groups of subcarriers i.e. clusters and each cluster is modulated independently rather than each subcarrier which reduces the computational complexity and feedback load of the adaptive scheme [53].

In the cluster-based adaptive modulation scheme, SNR is estimated at the receiver for each group of subcarriers (i.e. cluster). The received cluster SNR is used as the CSI to choose the adaptive allocation of the transmission parameters for each cluster, which are sent back to the transmitter for the next frame. If the received cluster SNR falls below the threshold, the data subcarriers in those clusters are considered as weak subcarriers and

discarded for the next transmission. Then the residual power is distributed among the remaining available subcarriers and the remaining available data subcarriers are transmitted with different modulation sizes depending on the received cluster SNR for the next data frame and thus higher data rate, better power and spectral efficiency can be achieved.

In the frame-based adaptive scheme, all subcarriers of one frame are modulated with one modulation size and in the cluster-based adaptive scheme, group of subcarriers (i.e. clusters) of one frame are modulated with different modulation sizes. Hence, the cluster-based adaptive modulation requires large amount of CSI feedback as different modulation sizes need to be fed back for the clusters for the next transmission. So, higher feedback rate is required for the cluster-based adaptive modulation compared with the frame-based adaptive modulation.

4.2 Adaptive Allocation of Transmission Parameters

A cluster consists of a group of adjacent subcarriers. When the channel changes slowly across frequency, neighbouring subcarriers have similar SNR. Hence, the same modulation size is allocated for the neighbouring subcarriers. In such case, it is not necessary to feed back the transmission parameters for each subcarrier. The feedback can be done for the group of subcarriers (cluster) i.e., the total number of bits that are fed back to the transmitter can be reduced resulting reduction in the computational load of the system [53, 75]. For this reason, cluster-based adaptive modulation is studied in this chapter.

One of the factors that deteriorates the BER performance of UA systems is the deep faded subcarriers of the UA OFDM system. As a result, a large amount of transmitting energy is wasted on the deep faded subcarriers [76]. In the cluster-based adaptive modulation scheme, depending on the received cluster SNR, the deep faded subcarriers (i.e. weak subcarriers) are discarded for the next transmission. That's how the subcarriers are adaptively chosen by the proposed cluster-based adaptive modulation system.

In contrary to the frame-based adaptive modulation scheme, received cluster SNR of each cluster of the current frame is used as CSI for choosing the transmission parameters for the next frame in the cluster-based adaptive modulation scheme. The clusters that are in a deep fade are discarded which means no data is transmitted and zero power is allocated for those discarded clusters and remaining clusters will transmit data with proper modulation size depending on the CSI (i.e. cluster received SNR). That's how the modulation sizes are adaptively chosen by the proposed cluster-based adaptive modulation system.

As zero power is allocated for the discarded data subcarriers, the total transmission power is reduced for the next transmission which affects the overall throughput of the system. To solve this issue, the residual power is distributed among the remaining data subcarriers of the next frame. That's how the power is adaptively allocated by the proposed cluster-based adaptive modulation system. So, the proposed cluster-based adaptive scheme enables the system to perform the following:

- Adaptive allocation of the modulation size.
- Adaptive allocation of the data subcarriers.
- Adaptive allocation of the power on the data subcarriers.

The proposed adaptive modulation scheme allows the system

i. to choose a proper modulation depending on the channel conditions to improve the system throughput under a fixed BER.
ii. to discard subcarriers that experience deep fade to improve the energy efficiency of the system.
iii. to distribute the residual power among the remaining subcarriers which ensures constant transmitted symbol energy in spite of the channel variation to achieve overall better throughput of the system.

In the cluster-based adaptive modulation, each cluster contains combination of five pilot and fifteen data subcarriers (i.e. active subcarriers). Figure 17 shows the cluster structure in a frame.

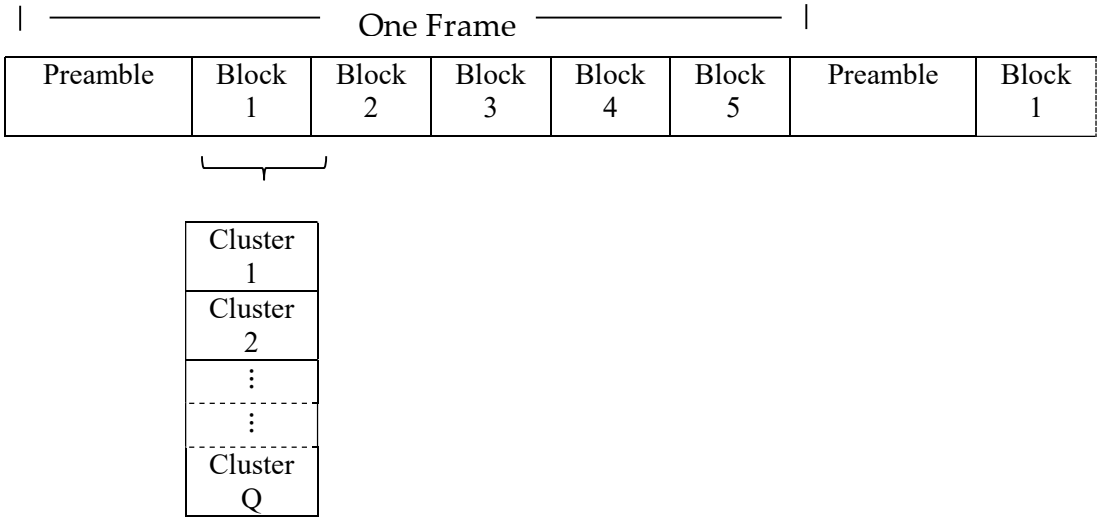

Figure 17: Cluster structure of the UA OFDM system.

The active subcarriers $\mathcal{K}_a$ where $\mathcal{K}_a = \mathcal{K}_p \cup \mathcal{K}_d$ [25] are grouped into Q clusters. The size of each cluster in each OFDM block is

$$C = \mathcal{K}_a/Q \, .$$

The SNR of each cluster in the frequency domain can be estimated as

$$\overline{\gamma_q} = \frac{\frac{1}{\overline{\mathcal{K}}_{a_q}} \sum_{m_q=1}^{\overline{\mathcal{K}}_{a_q}} \left| r_f[\mathcal{K}_{a_q}(m_q)] \right|^2}{\frac{1}{\overline{\mathcal{K}}_n} \sum_{m=1}^{\overline{\mathcal{K}}_n} \left| r_f[\mathcal{K}_n(m)] \right|^2} - 1 \tag{21}$$

where $\mathcal{K}_{a_q}$ is the set containing the indices of pilot and data subcarriers of the qth cluster. In the cluster-based adaptive modulation scheme, after estimating the received cluster SNR using (21), an algorithm is followed to discard and keep the clusters for the next transmission which is shown in Figure 18. If the received SNR of a cluster is less than the target SNR, then the data subcarriers of this cluster are discarded from the next transmitted frame. If the received SNR of a cluster is greater than the target SNR, we keep the data subcarriers of this cluster and send the adaptively allocated parameters for the next transmission to the transmitter.

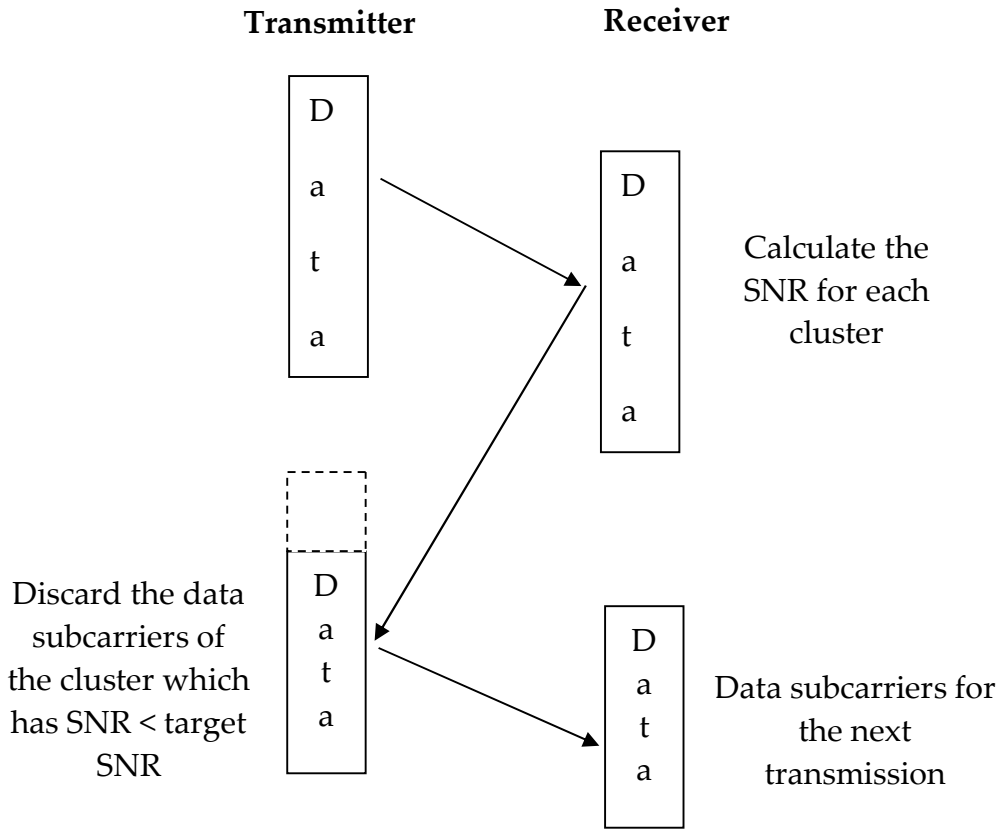

Figure 18: Discarding data subcarriers depending on the cluster SNR estimation.

After discarding the data subcarriers under a target SNR, the remaining OFDM data symbols in next frame are generated as

$$\boldsymbol{s_{remd}} = (s_d[1], \dots, s_d[\, K_{remd}])^T \tag{22}$$

where K_{remd} is the number of remaining data subcarriers in the next frame. The total power of the OFDM symbol is

$$P_{total} = P_{remd} + P_{res} \tag{23}$$

where P_{remd} is the power of the remaining data subcarriers and P_{res} is the power of the discarded subcarriers of the current frame.

As the data subcarriers under the target SNR are discarded, the total power of the data subcarriers is reduced for the next frame. To further improve the system performance, the residual power P_{res} is distributed among the remaining subcarriers for the next frame. After distributing P_{res} in the remaining subcarriers, the data symbols of the next frame is represented as

$$\boldsymbol{s_d} = \beta\ (s_d[1], \dots, s_d[\, K_{remd}])^T \tag{24}$$

where $\beta = \sqrt{K_d/K_{remd}}$ is the factor of the distribution of average power of the data subcarriers.

In this research, modulation size is fed back from the feedback link transmitter to the feedback link receiver. Receiving the right modulation size for the frames (frame-based) and clusters (cluster-based) is important. In the frame-based adaptive modulation only one modulation size is fed back for the next frame whereas in the cluster-based adaptive modulation Q modulation sizes need to be fed back for Q clusters of a frame. A successful modulation/ demodulation process of the forward channel entirely depends on the correct detection of modulation size at the feedback channel. To make the feedback link reliable and for errorless detection of the bits containing

modulation size, repetition code is considered at the feedback transmitter and majority voting is considered at the feedback receiver. At the feedback transmitter bits are repeated several times for each modulation size and the bits are recovered at the feedback receiver by searching the bit stream that occurs most often.

4.3 System Implementation

Like the frame-based adaptive modulation, a combination of NI LabVIEW software and CompactDAQ device are adopted for the real-time cluster-based adaptive modulation for UA OFDM communication systems.

4.3.1 System Hardware

An NI CompactDAQ system is used for signal generation and acquisition in our UA OFDM communication system. CompactDAQ is capable of analog I/O, digital I/O, counter/timer operations, and industrial bus communication. The following system hardware are used in the cluster-based adaptive UA OFDM system.

- NI cDAQ-9174 – transfer data between computer and I/O devices.
- NI-9260 – output signals to the transducer.
- NI-9232 – acquire signals from the hydrophone.
- CTG0052 – transmitter transducer.
- Reson Reference TC 4034 – receiver hydrophone.

4.3.2 Software Implementation

Like the frame-based adaptive modulation, the software of the proposed cluster-based adaptive UA OFDM system is designed and implemented using NI LabVIEW which is described in section 3.3.2. Unlike the frame-based adaptive modulation scheme, two Reson reference hydrophones are used in the cluster-based adaptive modulation experiment for both forward and feedback links. The real-time adaptive modulation scheme is shown in Figure 7 where transducer (a) and transducer (b) refer to the CTG0052 transducer, hydrophone (a) and hydrophone (b) refer to the Reson reference hydrophone.

4.4 Results and Discussions

In this section, the experimental results of the cluster-based adaptive modulation scheme are presented and discussed. The performance of the proposed cluster-based adaptive modulation scheme is verified through recent UA OFDM communication experiments performed in the Canning River, Western Australia.

4.4.1 Tank Experiment Results

In the cluster-based adaptive modulation scheme, data subcarriers are grouped into 22 clusters and the SNR is estimated for each cluster. After estimating the cluster SNR of the received signal, the weak clusters are discarded and the remaining clusters i.e. data subcarriers are selected for the next transmission with modulation sizes depending on the channel condition. Then the residual power is distributed among the remaining data

subcarriers for the next transmission. Thus the cluster-based adaptive modulation scheme adaptively choose the subcarriers, modulation size and allocate the power.

In the tank experiment, two CTG0052 transducers, two Reson reference hydrophones were used. In order to obtain the SNR thresholds for various modulation schemes under a target BER, we first perform one-way communication experiment with one pair of transducer and hydrophone. The received cluster SNR is changed through varying the power of the transmitted signal. The target SNR is chosen by plotting the average received cluster SNR vs BER results. After the SNR thresholds are obtained, the experiment of adaptive modulation is performed by placing another pair of transducer and hydrophone in the tank. Figure 19 shows the location of the transducers and hydrophones in the tank during the experiment. The length, width and depth of the tank are 2.5 m, 1.5m and 1.8 m respectively.

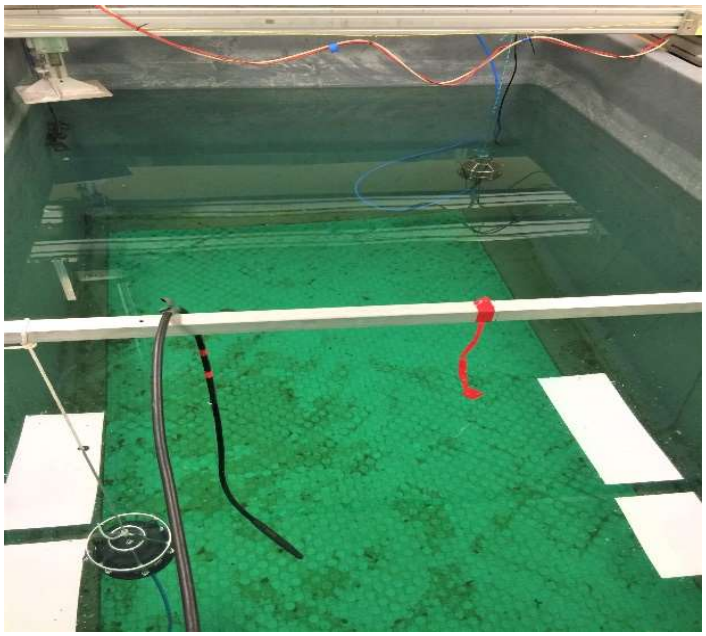

Figure 19 : Location of the transducers and hydrophones for forward and feedback links for the cluster-based adaptive modulation.

Table 8: Parameters used in the tank experiment of the cluster-based adaptive modulation.

Bandwidth	B = 4 kHz
Number of subcarriers	K_s = 512
Subcarrier spacing	f_{sc} = 7.8 Hz
Length of OFDM symbol	T = 128 ms
Length of CP	T_{cp} = 25 ms
Number of pilot subcarriers	K_p = 110
Number of data subcarriers	K_d = 330
Number of null subcarriers	K_n = 72

During the experiment, we bypassed the frequency offset estimation and compensation module in Figure 6 as the Doppler shift is very small in a tank. The system parameters used for the adaptive modulation schemes in the tank experiment are listed in Table 8.

Table 9 : Switching threshold for the cluster-based adaptive modulation scheme at target BER 0.01 in the tank experiment.

Mode	**Modulation**	**Threshold**
1	Discard	SNR < 3.7 dB (target SNR)
2	BPSK	3.7dB ≤ SNR < 7.5 dB
3	QPSK	7.5 dB ≤ SNR < 16.5 dB
4	16QAM	SNR ≥ 16.5 dB

For the tank experiment, the target uncoded BER is determined as 0.01 for the cluster-based adaptive modulation scheme. Switching thresholds that obtained from the fixed modulation experiment are listed in Table 9.

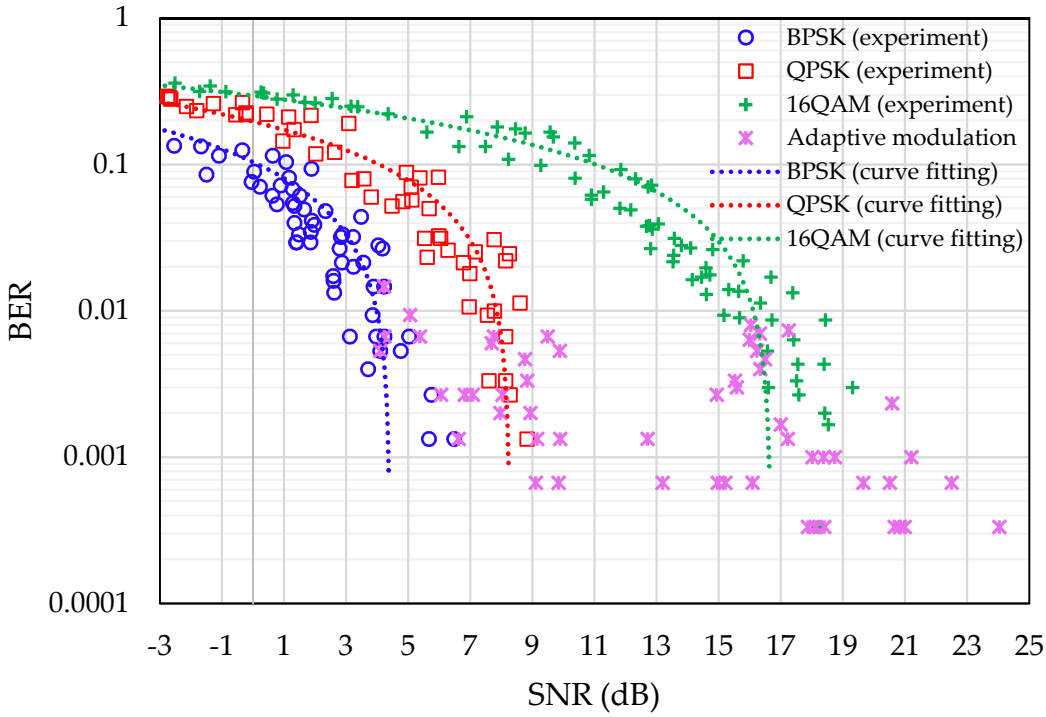

Figure 20: BER performance of the proposed cluster-based adaptive modulation scheme during the tank experiment.

Using Figure 20, the target SNR is selected to discard the deep faded clusters and a set of SNR thresholds are determined for switching the modulation mode for different remaining clusters. Figure 20 also shows the BER performance for the cluster-based adaptive modulation.

4.4.2 River Experiment Results

The performance of the proposed cluster-based adaptive modulation scheme is verified through recent UA OFDM communication experiments performed in the Canning River, Western Australia and the experimental results verify the superiority of the proposed adaptive scheme. In the river

experiment, two pair of CTG0052 transducers and Reson reference hydrophones were used for the forward link and feedback link. The system parameters used in the cluster-based river experiment are the same as the parameters used in the cluster-based tank experiment and are listed in Table 8. Figure 21 shows the location of the transducers and hydrophones in the river during the cluster-based adaptive modulation experiment. The distance between the forward link and the feedback link was around 7.5 m. The water depth along the direct path varied between 1 m to 1.2 m.

Figure 21**:** Location of the transducers and hydrophones in the river experiment for the cluster-based adaptive modulation.

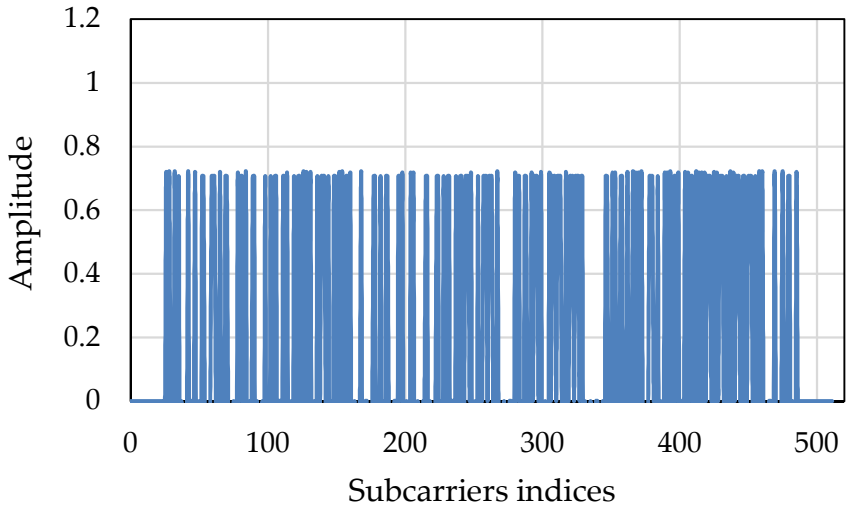

(a)

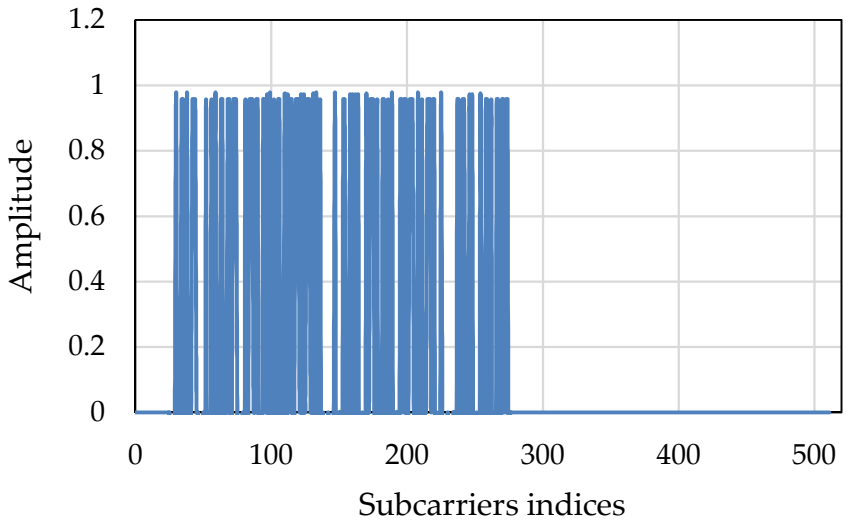

(b)

Figure 22: (a) Subcarrier amplitude when all clusters are available and (b) Subcarrier amplitude when 10 of the clusters are discarded.

During the river experiment, we bypassed the frequency offset estimation and compensation module in Figure 6 as there is no relative motion between the transmitter and receiver. In river experiment, firstly, the power allocation algorithm has been performed and verified as shown in Figure 22. Two frames were transmitted with modulation size 2 (QPSK). Figure 22 (a) shows that the first frame was transmitted keeping all clusters

(data subcarriers) available and Figure 22 (b) shows that the next frame was transmitted discarding almost half of the clusters (first 12 available clusters and last 10 discarded clusters). From Figure 22 (b), it can be seen that, the amplitude of the subcarriers is increased compared with Figure 22 (a) which means the residual power of the discarded data subcarriers is distributed among the remaining first 12 available clusters (data subcarriers) for the next transmission.

The distribution and allocation of the residual power among the remaining data subcarriers ensures constant transmitted symbol energy in spite of the channel variation. Figure 23 shows the estimated received SNR of the clusters in a frame. In the figure, the blue dots represent the SNRs when all the 22 clusters are available i.e. all the data subcarriers are carrying information and the green dots represent the SNRs when the last 10 clusters are discarded and the first 12 clusters are carrying information. It can be seen that the estimated cluster SNR of the first 12 clusters is higher than the estimated cluster SNR when all the clusters are available which also verifies the power allocation to the remaining data subcarriers.

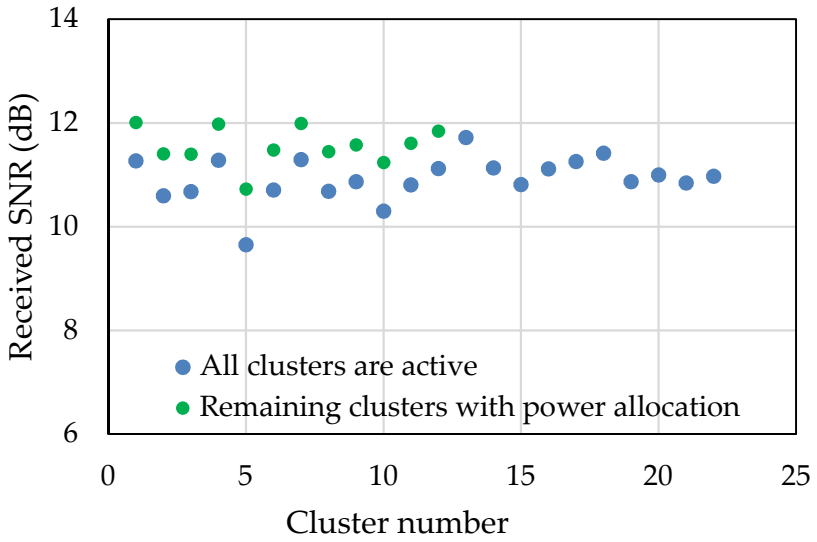

Figure 23**:** Estimated received SNR of the clusters of a frame.

Figure 24 shows the transmission symbol power with and without the adaptive power allocation algorithm during the river experiment. After discarding the deep faded data subcarriers if the residual power is not allocated among the remaining data subcarriers then the transmission power of the next frames fluctuates whereas if the residual power is allocated then the transmission power always keeps almost constant. In summary, it can be said that, when the channel condition is not good enough, the power allocation algorithm allocates more power on remaining available data subcarriers which ensures overall better throughput of the system.

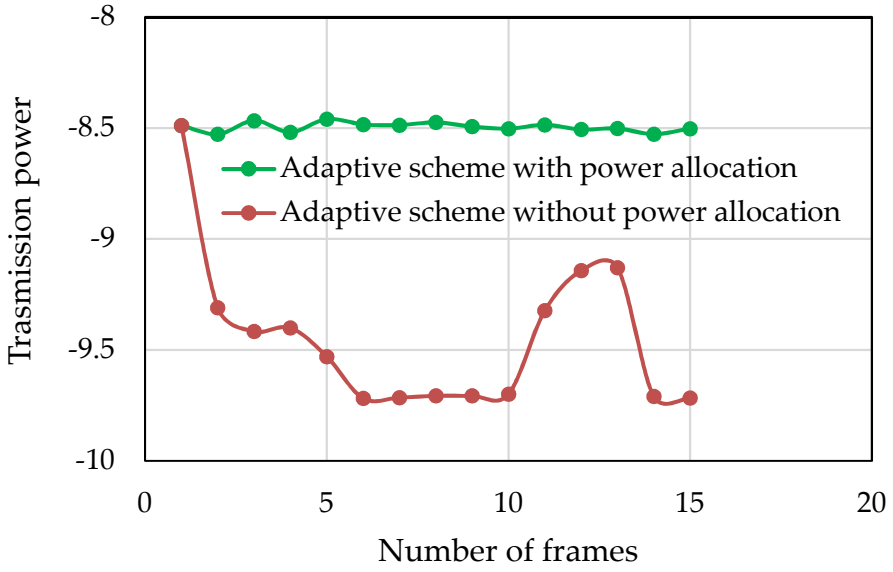

Figure 24**:** Transmitted symbol power for different channel conditions.

Table 10 : Switching thresholds for the cluster-based adaptive modulation scheme at target BER 0.01 in the river experiment.

Mode	**Modulation**	**Threshold**
1	Discard	SNR < 1 dB (target SNR)
2	BPSK	1 dB ≤ SNR < 5 dB
3	QPSK	5 dB ≤ SNR < 12 dB
4	16QAM	SNR ≥ 12 dB

For the river experiment, the target uncoded BER is determined as 0.01 for the cluster-based adaptive modulation scheme. Switching thresholds for the cluster-based adaptive modulation scheme are presented in Table 10. Using Figure 25, the target SNR is selected to discard the deep faded clusters and a set of SNR thresholds are determined for switching the modulation mode for different remaining clusters. Figure 25 also shows the BER performance for adaptive modulation.

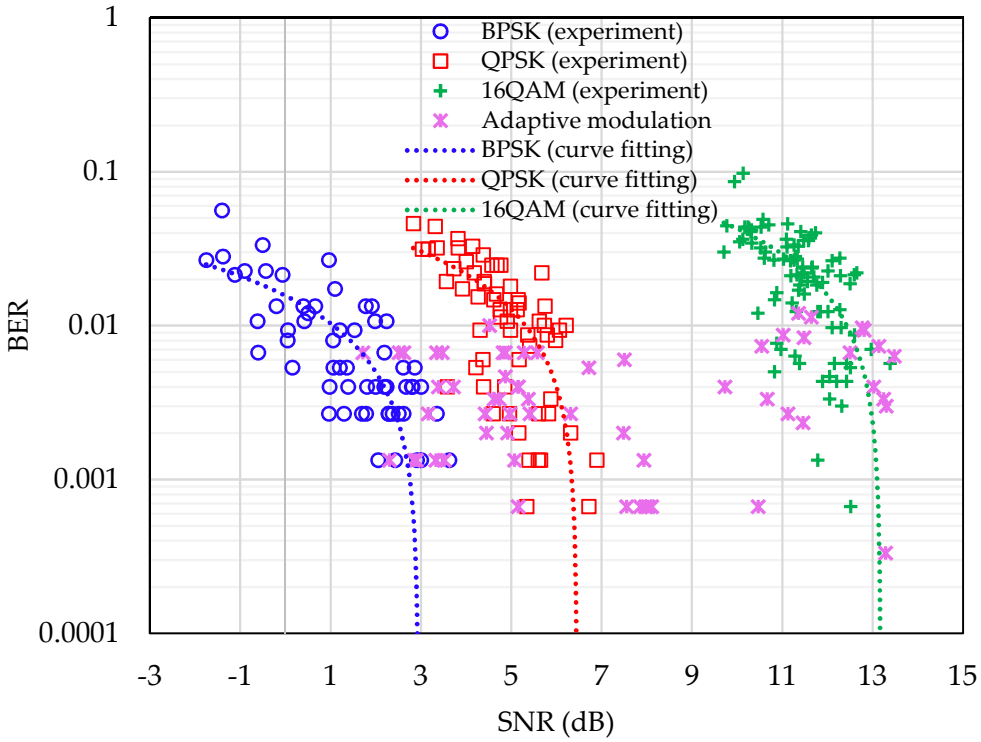

Figure 25: BER performance of the proposed cluster-based adaptive modulation scheme during the river experiment.

Figure 26 (a) and 26 (b) show the CFR of an OFDM block of a received frame and respective adaptively loaded bits in the clusters of that OFDM block for the next frame. It can be seen that the number of loaded bits i.e. modulation size for clusters are closely related to the CFR results. When the amplitude of the subcarrier cluster is higher the selected modulation size is also higher and vice versa. Figure 26 (c) shows the power distribution for the data subcarriers of the next OFDM block accordingly.

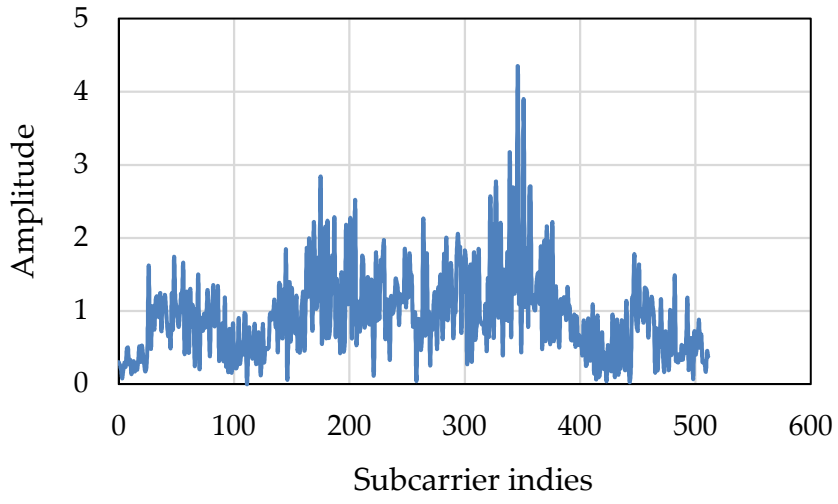

(a)

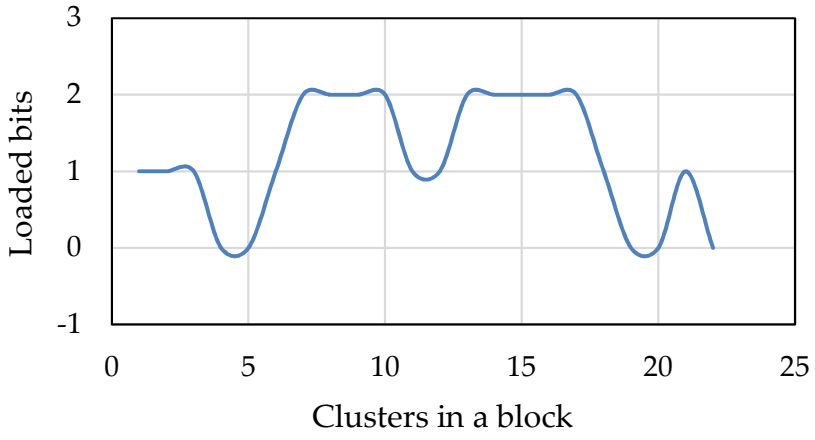

(b)

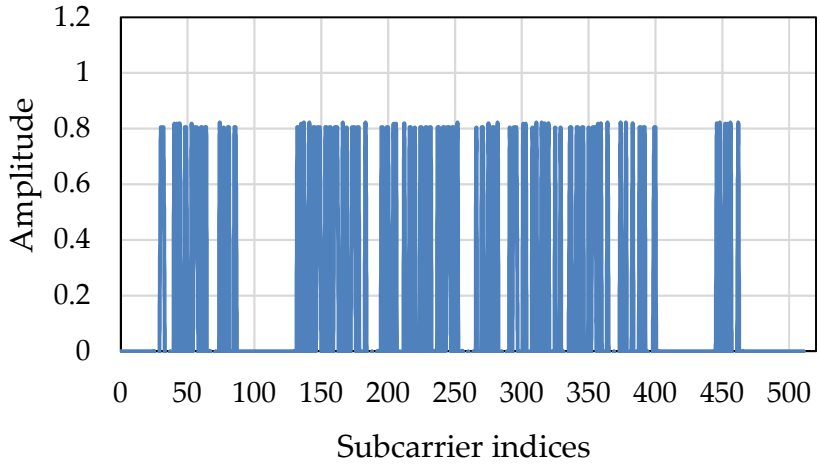

(c)

Figure 26**:** (a) CFR of the current OFDM block (b) Loaded bits of the next OFDM block according to (a). (c) Power distribution for the data subcarriers of the next OFDM block according to figure 26 (a).

Figure 27 shows the data rate of the proposed cluster-based adaptive modulation scheme. It can be seen that the data rate also increases with the increase of the transmit power. When the transmit power is low, the deep faded data subcarriers are discarded and data rate around the target SNR is lower whereas the data rate is higher when the residual power is distributed among the remaining subcarriers. In summary, it can be said that, the proposed cluster-based adaptive modulation adaptively allocate subcarriers, modulation size and power that improves the reliability of communication, improves the energy efficiency and ensures overall better throughput of the system.

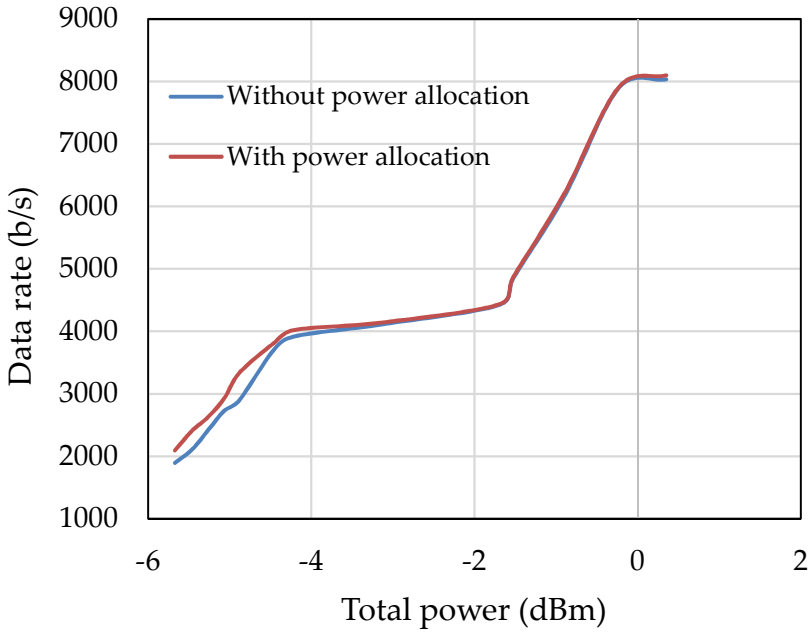

Figure 27**:** Data rate of the cluster-based adaptive modulation.

4.5 Conclusion

In the OFDM adaptive modulation system, the transmission parameters (i.e. modulation size) are fed back to the transmitter for the next transmission. If the transmission parameters are fed back for each subcarrier,

then the computation will become very complex and the feedback load will be very high. That's why the cluster-based adaptive modulation scheme is chosen where subcarriers are grouped into clusters in a frame. In the proposed cluster-based adaptive modulation scheme, 330 data subcarriers are grouped into 22 clusters. Therefore, 22 modulation sizes (i.e. transmission parameters) need to be fed back instead of 330 from the receiver to the transmitter which reduces the computational complexity and the feedback load. However, compared with the proposed frame-based adaptive modulation scheme, higher feedback rate is required for the cluster-based adaptive scheme, because in the frame-based adaptive scheme, all the subcarriers were modulated in the same manner i.e. only one modulation size needs to be fed back for all the subcarriers to the transmitter. So, to make the feedback link reliable and for errorless detection of the bits containing modulation size, repetition code and majority voting are considered at the feedback link of the cluster-based adaptive scheme.

The proposed cluster-based adaptive modulation scheme improves the system throughput under a fixed BER by choosing proper modulation sizes for clusters depending on the channel conditions, improves the energy efficiency of the system by discarding subcarriers that experience deep fade, achieves overall better throughput of the system by distributing the residual power among the remaining subcarriers which ensures constant transmitted symbol energy in spite of the channel variation. In summary, it can be said that the proposed cluster-based adaptive system is an energy efficient system which guarantees continuous connectivity and ensures higher data rate for a nonstationary time-varying UA channel.

Chapter 5

Conclusions and Future Work

In this chapter, the main conclusions of this work are summarized and some suggestions are discussed which can be considered for future work.

A real-time OFDM based adaptive UA communication system is studied in this research employing the NI LabVIEW software and NI CompactDAQ device. Limited bandwidth and time-varying multipath propagation place significant constraints on the achievable throughput of UA communication systems. OFDM adaptive modulation has received significant attention to increase the bandwidth efficiency and data rate of the UA system. The frame-based and the cluster-based adaptive modulation schemes are developed for UA OFDM communication systems in this research where the adaptation is done frame by frame. In the frame-based adaptive scheme, all subcarriers of one frame are modulated with one modulation size and in the cluster-based adaptive scheme, groups of subcarriers (i.e. clusters) of one frame are modulated with different modulation sizes.

The estimated received SNR and received cluster SNR is used as CSI for the frame-based and the cluster-based adaptive modulation system respectively. In the presence of ICI, both the actual noise power and the ICI are reflected in the SNR estimation. Hence, estimated SNR is chosen as the

performance metric for adaptive modulation for mode switching which reflects the channel variation as well as Doppler effects.

Most applications demand a certain minimum BER and an adaptive modulation scheme is designed to maintain a constant BER for all channel SNR i.e. for any channel condition. In this research, fixed modulation system based on BPSK, QPSK and 16QAM schemes are investigated in both the frame-based and cluster-based modulation scheme to choose the target BER to perform adaptive modulation.

5.1 Frame-Based Adaptive Modulation

In this research, a frame-based adaptive modulation scheme is proposed which ensures higher data rate and better spectral efficiency of the UA communication systems. Simulation and experimental results are presented in chapter 3 to demonstrate the effectiveness of the proposed frame-based adaptive scheme.

- In the frame-based adaptive modulation scheme, higher order modulations can be chosen for transmission depending on channel condition which enables the transmission of more bits per symbol and thus higher data rate and better spectral efficiency can be achieved.
- The simulation and experimental results prove that the highest modulation size is chosen under certain BER and SNR. Thus, a better tradeoff between data rate and overall BER is attained in the frame-based adaptive modulation.
- In the frame-based adaptive modulation scheme, all subcarriers of the data frame are modulated in the same manner. So, the

frame-based adaptive modulation requires less amount of CSI feedback as only one modulation size needs to be fed back for each frame for the next transmission. Hence, compared with the cluster-based scheme, it requires low feedback rate, which makes it more robust than the cluster-based scheme.

5.2 Cluster-Based Adaptive Modulation

UA channel is time-varying and some subcarriers of the OFDM system may be subject to a deep fading. To mitigate this effect, subcarrier-based adaptive modulation scheme is chosen where each subcarrier or group of subcarriers (i.e. cluster) can be modulated independently. In this research, a cluster-based adaptive modulation scheme is proposed which allows the system to select subcarriers, modulation size and distribute power adaptively. The proposed cluster-based adaptive system is an energy efficient and reliable communication system which improves the energy efficiency of the system, ensures higher data rate and guarantees continuous connectivity for a nonstationary time-varying UA channel. The experimental results are presented in chapter 4 to demonstrate the effectiveness of the proposed cluster-based adaptive scheme.

- The proposed cluster-based adaptive modulation scheme improves the system throughput under a fixed BER by choosing proper modulation sizes for clusters depending on channel conditions.
- The proposed cluster-based adaptive modulation improves the energy efficiency of the system by discarding subcarriers that experience deep fade.

- The proposed cluster-based adaptive modulation ensures constant transmitted symbol energy in spite of the channel variation and achieves overall better throughput of the system by distributing the residual power among the remaining subcarriers.

In the cluster-based adaptive modulation scheme, subcarriers are grouped into clusters to reduce the computational and feedback load and each cluster is independently modulated. Therefore, higher feedback rate is required. To make the feedback link reliable and for errorless detection of the bits containing modulation size, repetition coding and majority voting are considered at the feedback link.

5.3 Future Work

Some adaptive modulation schemes and experiments have been left for the future due to lack of time as experiments with real data are usually very time consuming. Even it required days to prepare and conduct a trial and process the collected data. Different transmission parameters for adaption, deeper analysis of the feedback channel, new proposals to try different methods can be considered in future research. There are some ideas described below that could be tested:

In this research, different transmission parameters such as subcarriers, modulation sizes are adaptively allocated and the residue power is adaptively distributed for the next transmission. In future work, more transmission parameters can be considered to allocate adaptively for the next transmission. In UA communication, the reflection from water surfaces and bottoms and obstacles causes very long delay spread which is large

compared to the symbol duration leading to a phenomenon ISI. The severity of ISI increases with the length of delay spread. The CP is used as a guard that protects against interference from previously transmitted symbols where CP length needs to be longer than the delay spread. In future CP length can be considered as an adaptively allocated transmission parameter. At first, the transmission will commence with a long CP length to make sure that the OFDM symbol is free from ISI. Then if the estimated delay spread is much shorter than the current CP length, a shorter CP length can be allocated for the next transmission.

In this research, the residual power is distributed among the remaining clusters of the frame for the next transmission in the cluster-based adaptive modulation system. In future research, the transmitted power level can be allocated for each cluster. As different clusters experience different fading, the transmit power levels can be allocated accordingly. Depending on the instantaneous fading characteristics, the power level can be allocated on each cluster. After adopting power allocation algorithm, the system will be able to achieve higher data rate with the same feedback data compared with the proposed schemes. However, the transmitter requires more complex design to allocate different power levels for each cluster.

Developing a channel predictor can be considered in the future to make the adaptive modulation schemes more successful. An accurate channel prediction can be carried out successfully if frequency offset estimation and compensation are done properly. A proper Doppler compensation ensures the stability over intervals of time that are long enough to support channel prediction at least several seconds ahead [61, 65]. The delay is unavoidable in UA scenario. Hence, the CSI that is obtained for the next transmission can be outdated. However, based on the previous CSI, channel gain prediction

algorithm can be developed which will help the system to predict the channel at least a travel time ahead.

Appendix

CTG0052

The CTG0052 transducer used in our system is from SonoTube Series – Communication Transducers, Chelsea technologies. The transmit sensitivity of the CTG0052 transducer is shown in Figure 28 which is used to determine the carrier frequency and bandwidth of the system [40].

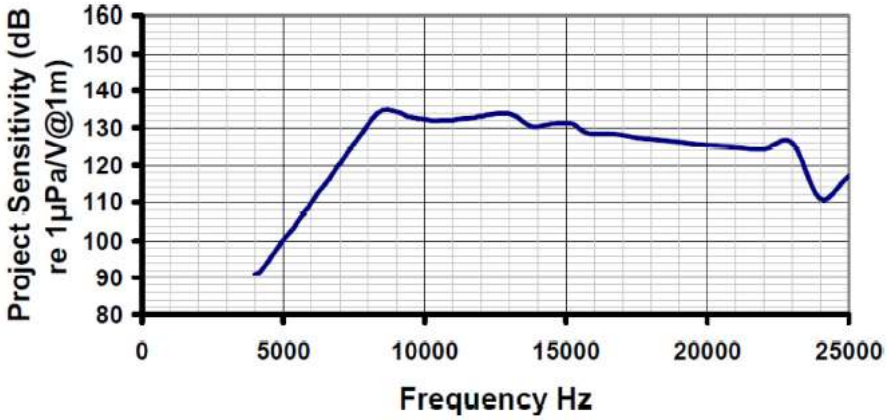

Figure 28**:** Transmit sensitivity of the CTG0052 transducer

HTI-96-Min

The HTI-96-Min portable hydrophone from High Tech Inc., Long Beach, MS, USA, is widely applied in UA communication systems. The specification of the hydrophone is listed in Table 11.

Table 11: The specification of the HTI-96-Min hydrophone.

Sensitivity	Without Pre-Amp:	-201 dB re: 1V/µPa (8.9 V/bar)
	With Pre-Amp:	Max -165 dB re: 1V/µPa (562 V/bar)
		Min -240 dB re: 1V/µPa (0.1V/bar)
Frequency Response		2 Hz to 30 kHz
Preamplifier Type		Voltage Mode Current Mode

Reson Reference TC 4034

The TC4034 broad band spherical hydrophone provides uniform omnidirectional characteristics over a wide frequency range of 1Hz to 480 kHz. The specification of the hydrophone is given below. The receiving sensitivity of the TC 4034 is shown in Figure 29.

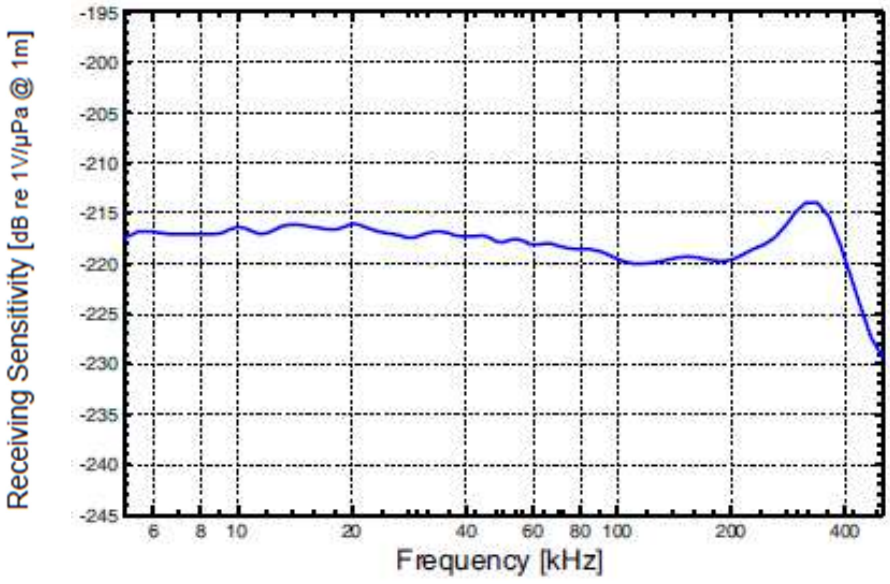

Figure 29**:** Receiving sensitivity of Reson Reference TC 4034 hydrophone.

Matching Network

The CTG0052 transducer is connected through a power amplifier and matching network to one of the channel of the NI-9260 module for transmitting UA communication signals. Figure 30 shows the schematic diagram of the matching network.

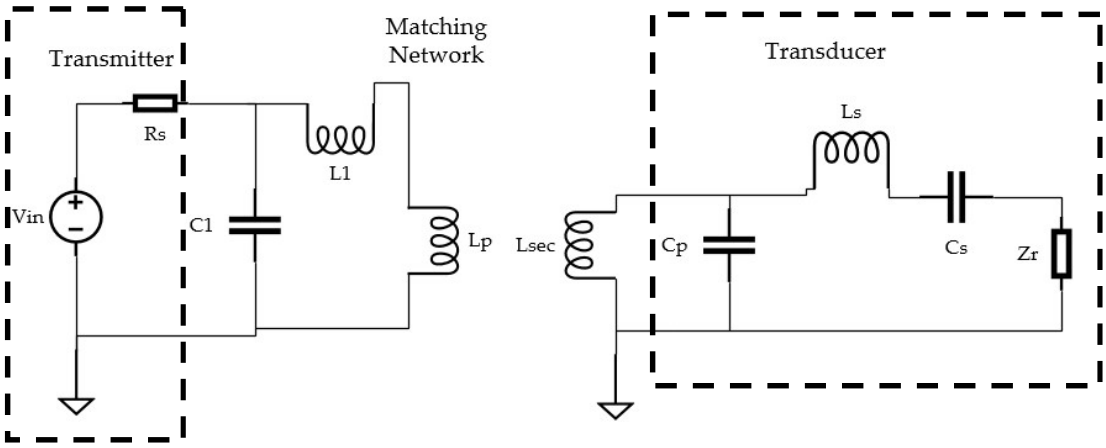

Figure 30: Schematic diagram of the Matching network.

Bibliography

1. M. Chitre, S. Shahabudeen, and M. Stojanovic, "Underwater acoustic communications & networking: Recent advances and future challenges", *Marine Technology Society Journal,* vol. Spring 2008, pp. 103-116, 2008.

2. J. Catipovic, M. Deffenbaugh, L. Freitag, and D. Frye, "An acoustic telemetry system for deep ocean mooring data aquisition and control", in *Proc. of MTS/IEEE OCEANS Conference*, Seatle, WA, Oct. 1989.

3. Y. R. Zheng, C. Xiao, T. C. Yang, and W. B. Yang, "Frequency-domain channel estimation and equalization for shallow-water acoustic communications", *Physical Communication*, vol. 3, pp. 48–63, Mar. 2010.

4. J. Tao, Y. R. Zheng, C. Xiao, and T. C. Yang, "Robust MIMO underwater acoustic communications using turbo block decision-feedback equalization", *IEEE Journal of Oceanic Engineering*, vol. 35, no. 4, pp. 948–960, Oct. 2010

5. A. Song, M. Badiey, A. E. Newhall, J. F. Lynch, H. A. DeFerrari, and B. G. Katsnelson, "Passive time reversal acoustic communications through shallow-water internal waves", *IEEE Journal of Oceanic Engineering*, vol. 35, no. 4, pp. 756–765, Oct. 2010

6. H. Wan, R.-R. Chen, J. W. Choi, A. Singer, J. Preisig, and B. FarhangBoroujeny, "Markov chain Monte Carlo detection for frequency-selective channels using list channel estimates", *IEEE Journal of Selected Topics in Signal Processing*, vol. 5, no. 8, pp. 1537–1547, Dec. 2011

7. L. E. Freitag, M. Stojanovic, S. Singh, and M. Johnson, "Analysis of channel effects on direct-sequence and frequency-hopped spread-

spectrum acoustic communications", *IEEE Journal of Oceanic Engineering*, vol. 26, no. 4, pp. 586-593, 2001.

8. M. Stojanovic and J. Preisig, "Underwater acoustic communication channels: Propagation models and statistical characterization", *IEEE Communications Magazine*, vol. 47, no. 1, pp. 84-89, Jan. 2009.

9. M. Badiey, Y. Mu, J. A. Simmen, and S. E. Forsythe, "Signal variability in shallow-water sound channels", *IEEE Journal of Oceanic Engineering*, vol. 25, no. 4, pp. 492–500, Oct. 2000.

10. A. Song, M. Badiey, H.-C. Song, W. S. Hodgkiss, M. B. Porter, and the KauaiEx Group, "Impact of ocean variability on coherent underwater acoustic communications during the kauai experiment (KauaiEx)", *The Journal of the Acoustical Society of America*, vol. 123, no. 2, pp. 856–865, 2008.

11. D. B. Kilfoyle and A. B. Baggeroer, "The state of the art in underwater acoustic telemetry" *IEEE Journal of Oceanic Engineering*, vol. 25, no. 1, pp. 4-27, Jan. 2000.

12. M. Stojanovic, "Recent advances in high-speed underwater acoustic communications", *IEEE Journal of Oceanic Engineering*, vol. 21, no. 2, pp. 125-136, Apr. 1996.

13. W. Q. Zhu, "Underwater acoustic communication system of AUV", *IEEE Oceanic Engineering Society. OCEANS'98. Conference Proceedings*, vol. 1, pp. 477-481, 1998.

14. M. Stojanovic, J.A. Catipovic, and J.G. Proakis, "Phase-coherent digital communications for underwater acoustic channels", *IEEE Journal of Oceanic Engineering*, vol. 19, no. 1, pp. 100-111, Jan. 1994.

15. Z. Xu, Y. V. Zakharov, and V. P. Kodanev, "Space-time signal processing of OFDM signals in fast-varying underwater acoustic channel", *OCEANS 2007 - Europe*, pp. 1-6, 2007.

16. M. Stojanovic "OFDM for underwater acoustic communications: Adaptive synchronization and sparse channel estimation", *in 2008 IEEE International Conference on Acoustics, Speech and Signal Processing, pp. 5288-5291*, 2008.

17. W. Yonggang, "Underwater acoustic channel estimation for pilot based OFDM", *2011 IEEE International Conference on Signal Processing, Communications and Computing (ICSPCC)*, pp. 1-5, 2011.

18. C. R. Berger, S. Zhou, J. Preisig, and P. Willett, "Sparse channel estimation for multicarrier underwater acoustic communication: From subspace methods to compressed sensing", *IEEE Trans. Signal Processing*, vol. 58, no. 3, pp. 1708–1721, Mar. 2010.

19. P. Carrascosa and M. Stojanovic, "Adaptive channel estimation and data detection for underwater acoustic MIMO OFDM systems", *IEEE Journal of Oceanic Engineering*, vol. 35, no. 3, pp. 635–646, Jul. 2010.

20. B. Li, J. Huang, S. Zhou, K. Ball, M. Stojanovic, L. Freitag, and P. Willett, "MIMO-OFDM for high rate underwater acoustic communications", *IEEE Journal of Oceanic Engineering*, vol. 34, no. 4, pp. 634–644, Oct. 2009.

21. B. Li, S. Zhou, M. Stojanovic, L. Freitag, and P. Willett, "Multicarrier communication over underwater acoustic channels with non-uniform Doppler shifts", *IEEE Journal of Oceanic Engineering*, vol. 33, no. 2, pp. 198–209, Apr. 2008.

22. M. Stojanovic, "Low complexity OFDM detector for underwater channels", in Proc. MTS/IEEE OCEANS Conference, Boston, MA, USA, Sep. 18–21, 2006.

23. T. Kang and R. Iltis, "Iterative carrier frequency offset and channel estimation for underwater acoustic OFDM systems", *IEEE Journal on Selected Areas in Communications*, vol. 26, no. 9, pp. 1650–1661, Dec. 2008.

24. T. Kang, H. C. Song, W. S. Hodgkiss, and J. S. Kim, "Long-range multi-carrier acoustic communications in shallow water based on iterative sparse channel estimation", The Journal of the Acoustical Society of America, vol. 128, no. 6, Dec. 2010.

25. S. Zhou and Z. Wang, "OFDM for underwater acoustic communications", John Wiley & Sons Ltd, 2014.

26. F. Frassati, C. Lafon, P. A. Laurent, and J. M. Passerieux, "Experimental assessment of OFDM and DSSS modulations for use in

littoral waters underwater acoustic communications", *Europe Oceans 2005,* vol. 2, pp. 826-831.

27. L. Freitag, M. Grund, S. Singh, J. Partan, P. Koski, and K. Ball, "The WHOI Micro-Modem: An acoustic communications and navigation system for multiple platforms," in *Proc. of OCEANS 2005 MTS/IEEE,* vol. 2, pp. 1086-1092, 2005.

28. B. Benson, G. Chang, D. Manov, B. Graham, and R. Kastner, "Design of a low-cost acoustic modem for moored oceanographic applications", in *Proc. of the ACM International Workshop on UnderWater Networks (WUWNet)*, Los Angeles, CA, Sep. 2006.

29. T. Fu, D. Doonan, C. Utley, R. Iltis, R. Kastner, and H. Lee, "Design and development of a software-defined underwater acoustic modem for sensor networks for environmental and ecological research", in *Proc. of MTS/IEEE OCEANS 2006*, Boston, MA, pp. 1-6, Sep. 2006.

30. E. Sozer and M. Stojanovic, "Reconfigurable acoustic modem for underwater sensor networks", in *Proc. of the ACM International Workshop on UnderWater Networks (WUWNet)*, Los Angeles, CA, Sep. 2006.

31. J. Wills, W. Ye, and J. Heidemann, "Low-power acoustic modem for dense underwater sensor networks", in *Proc. of the ACM International Workshop on UnderWater Networks (WUWNet)*, Los Angeles, CA, Sep. 2006.

32. F. Tong, S. Zhou, B. Benson, and R. Kastner, "R & D of dual mode acoustic modem test bed for shallow water channels", in *Proc. of the ACM International Workshop on UnderWater Networks (WUWNet)*, Woods Hole, MA, Sep. 30 - Oct. 1 2010.

33. H. Yan, L. Wan, S. Zhou, Z. Shi, J.-H. Cui, J. Huang, and H. Zhou, "DSP based receiver implementation for OFDM acoustic modems", *Elsevier Journal on Physical Communication*, vol. 5, no. 1, pp. 22–32, 2012.

34. H. Yan, S. Zhou, Z. Shi, and B. Li, "A DSP implementation of OFDM acoustic modem", in *Proc. of the ACM International Workshop on UnderWater Networks (WUWNet)*, Montr´eal, Qu´ebec, Canada, September 14, 2007.

35. Z. Yan, J. Huang, and C. He, "Implementation of an OFDM underwater acoustic communication system on an underwater vehicle with multiprocessor structure", in *Frontiers of Electrical and Electronic Engineering in China*, vol. 2, pp. 151–155, 2007.

36. L. Wan, Z.-H. Wang, S. Zhou, T.C. Yang, and Z. Shi, "Performance Comparison of Doppler Scale Estimation Methods for Underwater Acoustic OFDM", *Journal of Electrical and Computer Engineering, Special Issue on Underwater Communication and Networking*, 2012.

37. Wan, Lei, "Underwater acoustic OFDM: algorithm design, DSP implementation, and field performance", *Doctoral Dissertations*, 2014

38. H. S. Dol, P. Casari, T. van der Zwan, and R. Otnes, "Software-defined underwater acoustic modems: Historical review and the NILUS approach", *IEEE Journal of Oceanic Engineering*, vol. 42, no. 3, pp. 722–737, Jul. 2017.

39. P. Chen, Y. Rong, S. Nordholm, A. Duncan and Z. He, "A LabVIEW based implementation of real-time underwater acoustic OFDM system", *23rd Asia-Pacific Conference on Communications*, pp. 1-5, Dec. 2017.

40. P. Chen, Y. Rong, S. Nordholm, and Z. He, "An underwater acoustic OFDM system based on NI CompactDAQ and LabVIEW", *IEEE Systems Journal*, vol. 13, pp. 3858-3868, Dec. 2019.

41. K. Pelekanakis, L. Cazzanti, G. Zappa and J. Alves, "Decision tree-based adaptive modulation for underwater acoustic communications", *2016 IEEE Third Underwater Communications and Networking Conference (UComms)*, pp. 1-5, 2016.

42. M. Sadeghi, M. Elamassie and M. Uysal, "Adaptive OFDM-based acoustic underwater transmission: System design and experimental verification", *2017 IEEE International Black Sea Conference on Communications and Networking (BlackSeaCom)*, Istanbul, pp. 1-5, 2017.

43. J. A. Catipovic, "Performance limitations in underwater acoustic telemetry", *IEEE Journal of Oceanic Engineering*, vol. 15, no. 3, pp. 205-216, 1990.

44. E. Lawrey, "The suitability of OFDM as a modulation technique for wireless telecommunications, with a CDMA comparison." James Cook University, 1997.

45. B. Muquet, Z. Wang, and G. Giannakis, "Cyclic prefix or zero padding for wireless multicarrier transmissions?", *IEEE Trans. on Communication Technology*, vol. 50, no. 12, pp. 2136-2148, Dec. 2002.

46. L. Wan, H. Zhou, X. Xu, Y. Huang, S. Zhou, Z. Shi, and J.H. Cui, "Adaptive modulation and coding for underwater Acoustic OFDM", *IEEE Journal of Oceanic Engineering*, vol. 40, issue 2, pp. 327-336, Apr. 2015.

47. S. Mason, C. R. Berger, S. Zhou, and P. Willett, "Detection, synchronization, and Doppler scale estimation with multicarrier waveforms in underwater acoustic communication", *IEEE Journal on Selected Areas in Communications*, vol. 26, no. 9, pp. 1638-1649, Dec. 2008.

48. B. S. Sharif, J. Neasham, O. R. Hinton, and A. E. Adams, "Computationally efficient Doppler compensation system for underwater acoustic communications", *IEEE Journal of Oceanic Engineering*, vol. 25, no. 1, pp. 52–61, 2000.

49. U. Tureli and H. Liu, "A high-efficiency carrier estimator for OFDM communications", *IEEE Communication Letters*, vol. 2, no. 4, pp. 104–106, Apr. 1998.

50. M. Huang, S. Sun, E. Cheng, X. Kuai, and X. Xu, "Joint interference mitigation with channel estimated in underwater acoustic OFDM system", *TELKOMNIKA*, vol. 11, no. 12, pp. 7423-7430, 2013.

51. M. Chitre, M. Stojanovic, S. Shahabudeen and L. Freitag, "Recent advances in underwater acoustic communications & networking", in *Proc. IEEE Oceans'08 Conference*, Quebec City, Canada, Sept. 2008.

52. F. Zhong and W. Zhou. "Evaluation of channel estimation algorithms in OFDM underwater acoustic communications", *in Proceedings of the 10th International Conference on Underwater Networks & Systems (WUWNET '15),* New York, NY, USA, Article 8, page 1–2, Oct. 2015.

53. A. Radosevic, R. Ahmed, T. M. Duman, J. G. Proakis, and M. Stojanovic, "Adaptive OFDM modulation for underwater acoustic

communication: Design considerations and experimental results", *IEEE Journal of Oceanic Engineering*, vol. 39, no. 2, pp. 357-370, Apr. 2014.

54. S. Mani, T. M. Duman, and P. Hursky, "Adaptive coding/modulation for shallow-water UWA communications," in *Acoustics'08 Conference*, Paris, France, July 2008.

55. B. Tomasi, L. Toni, L. Rossi, and M. Zorzi, "Performance study of variablerate modulation for underwater communications based on experimental data," in *Proc. of MTS/IEEE OCEANS Conference*, Seattle, WA, USA, pp. 1–8, 2010.

56. P.S. Chow, J. M. Cioffi, and J. A. C. Bingham, "A practical discrete multitone transceiver loading algorithm for data transmission over spectrally shaped channels", *IEEE Trans.* on Communication, pp. 773-75, April, 1995.

57. S. K. Lai, R. S. Cheng, K. B. Letaief, and C. Ying Tsui , "Adaptive Tracking of Optimal Bit and Power Allocation for OFDM Systems in Time-Varying Channels" *IEEE Wireless Communications and Networking Conference*, vol. 2, pp. 776-780. 1999.

58. X. Shen, H. Wang, Y. Zhang, and R. Zhao, "Adaptive technique for underwater acoustic communication", *InTech*, 2012.

59. X. Cheng, M. Wen, X. Cheng, L. Yang, and Zhengyuan Xu, "Effective self-cancellation of intercarrier interference for OFDM underwater acoustic communications", *in proc. of the Eighth ACM International Conference on Underwater Networks and Systems (WUWNet '13)*, NY, USA, Article 33, 1–5, 2013.

60. L. Liu, S. Zhou, and J. Cui, "Prospects and problems of wireless communications for underwater sensor networks", *Wireless Communication Mobile Computing,* vol. 8, pp. 977–994, 2008.

61. A. Radosevic, T. M. Duman, J. G. Proakis, and M. Stojanovic "Channel prediction for adaptive modulation in underwater acoustic communications", *OCEANS 2011 IEEE*, pp. 1-5, Santander, Spain, Jun. 2011.

62. K. Xiao-Yan, S. Hai-xin , Q. Jie and C. En, "CSI feedback-based CS for underwater acoustic adaptive modulation OFDM system with channel

prediction" , *China Ocean Engineering*, vol. 28, no. 3, pp. 391 – 400, Jun. 2014.

63. P. Chen, Y. Rong and S. Nordholm, "Forward-backward block-wise channel tracking in high-speed underwater acoustic communication", *OCEANS 2015*, pp. 1-5, Washington DC, Oct. 1015.

64. T. C. Yang, "Properties of underwater acoustic communication channels in shallow water", *The Journal of the Acoustical Society of America,* vol. 131, no. 1, pp.129-145, Jan. 2012.

65. B. Li, "Multicarrier modulation for underwater acoustic communication", *PhD thesis*, University of Connecticut, 2009.

66. P. Chen, Y. Rong, S. Nordholm, Z. He, and A. Duncan, "Joint channel estimation and impulsive noise mitigation in underwater acoustic OFDM communication systems", *IEEE Trans. Wireless Communication*, vol. 16, pp. 6165-6178, Sep. 2017.

67. P. Chen, Y. Rong, S. Nordholm, and Z. He, "Joint channel and impulsive noise estimation in underwater acoustic OFDM systems," *IEEE Transactions on Vehicular Technology*, vol. 66, pp. 10567-10571, Nov. 2017.

68. S. Guo, Z. He, W. Jiang, Y. Ou, K. Niu, Y. Rong, M. Caley and A. J. Duncan, "Channel estimation based on compressed sensing in high-speed underwater acoustic communication", *2013 9th International Conference on Information, Communications & Signal Processing*, pp. 1-5, 2013.

69. U Tureli, H Liu, and MD Zoltowski. "OFDM blind carrier offset estimation: ESPRIT", *IEEE Trans. on Communications*, vol. 48, no. 9, pp. 1459-1461, 2000.

70. C. L. Liu and K. Feher, "Pilot-symbol aided coherent M-ary PSK in frequency-selective fast Rayleigh fading channels", in *IEEE Trans. on Communications*, vol. 42, no. 1, pp. 54-62, Jan. 1994,

71. X. Wang,, X. Wang, R. Jiang, W. Wang, Q. Chen, and X Wang, "Channel modelling and estimation for shallow underwater acoustic OFDM communication via simulation platform", *Applied Sciences*, vol. 9, no. 3, pp. 447, 2009.

72. M. Chitre, "A high-frequency warm shallow water acoustic communications channel model and measurements", *The Journal of the Acoustical Society of America*, vol. 122, no. 5, pp. 2580–2586, 2007.

73. A. Svensson, "An Introduction to adaptive QAM modulation schemes for known and predicted channels", in *proc. of the IEEE*, vol. 95, no. 12, pp. 2322-2336, Dec. 2007.

74. J. Faezah and K. Sabira, "Adaptive modulation with OFDM system", *International Journal of Communication Networks and Information Security*, vol. 1, no. 2, Aug. 2009.

75. A. Radosevic, T. M. Duman, J. G. Proakis, and M. Stojanovic, "Adaptive OFDM for underwater acoustic channels with limited feedback", *2011 Conference Record of the Forty Fifth Asilomar Conference on Signals, Systems and Computers*, pp. 975-980, Nov. 2011.

76. Y. Luo, S. Hu, C. Feng, and J. Tong, "Power optimization algorithm for OFDM underwater acoustic communication using adaptive channel estimation", Journal of the Systems Engineering and Electronics, vol. 30, no. 4, pp.662 – 671, Aug. 2019.